Gravitational Waves: the Science of Einstein Telescope

Michele Maggiore

UNIVERSITÉ DE GENÈVE
FACULTÉ DES SCIENCES
Département de physique théorique

Giornate di Studio Piano Triennale INFN 2026-2028
Perugia, 7-8 luglio , 2025

Exploring the Universe with gravitational waves

- first direct detection of GWs by the LIGO-Virgo Collaboration in 2015 after 50+ yr of developments

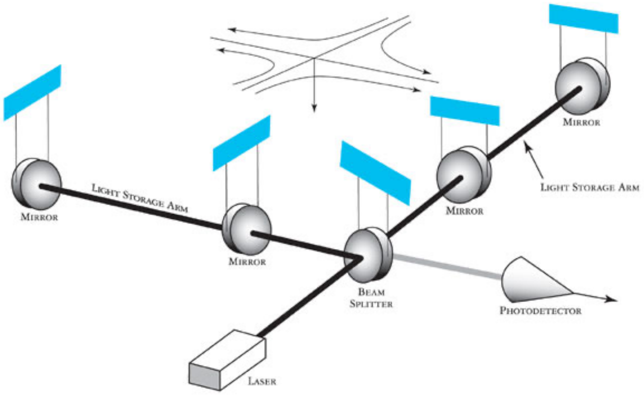

First detection of a BH-BH coalescence, Sept. 14, 2015

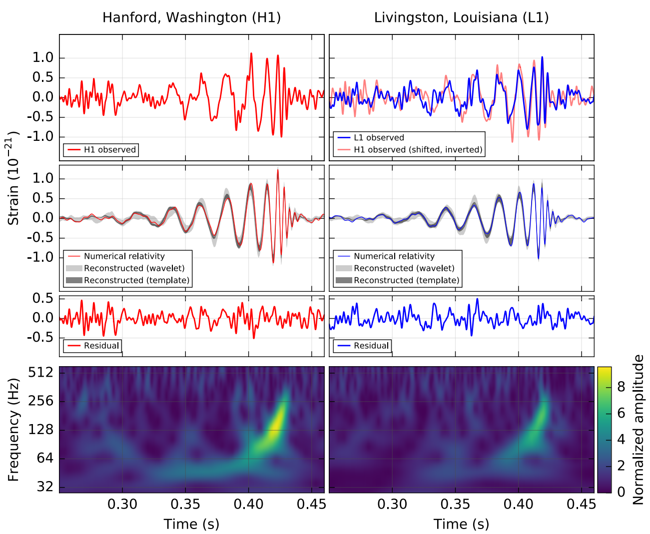

parameter estimation from matched filtering:

primary BH mass	$36^{+5}_{-4}\,M_\odot$
secondary BH mass	$29^{+4}_{-4}\,M_\odot$
final BH mass	$62^{+4}_{-4}\,M_\odot$
final BH spin $\hat{a} \equiv Jc/(GM^2)$	$0.67^{+0.05}_{-0.07}$
luminosity distance	410^{+160}_{-180} Mpc
source redshift	$0.09^{+0.03}_{-0.04}$

3 solar masses radiated in GWs in a few ms !!

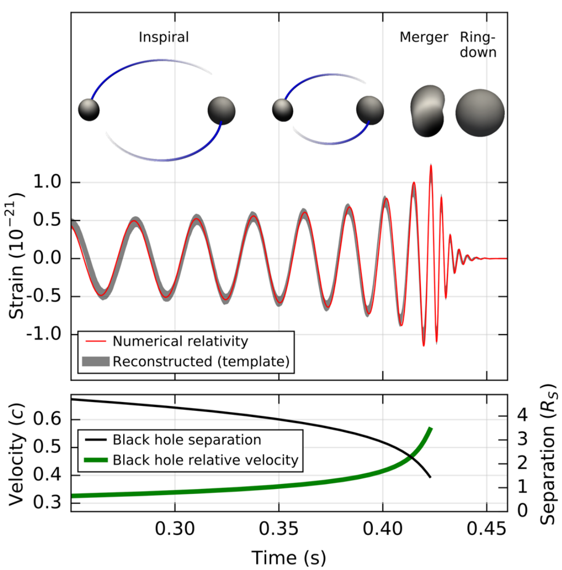

v/c ~ 0.4 at merger !

Nobel Prize 2017

Another milestone was the first NS-NS binary, GW170817

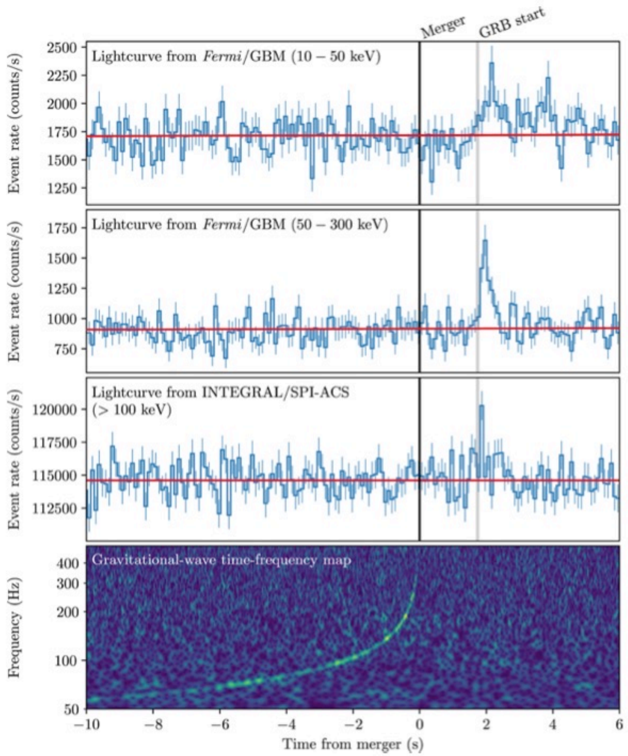

Observed in coincidence with a GRB

detection and follow-up of the counterpart in all wavelengths of the EM spectrum

⇒ multi-messenger astronomy

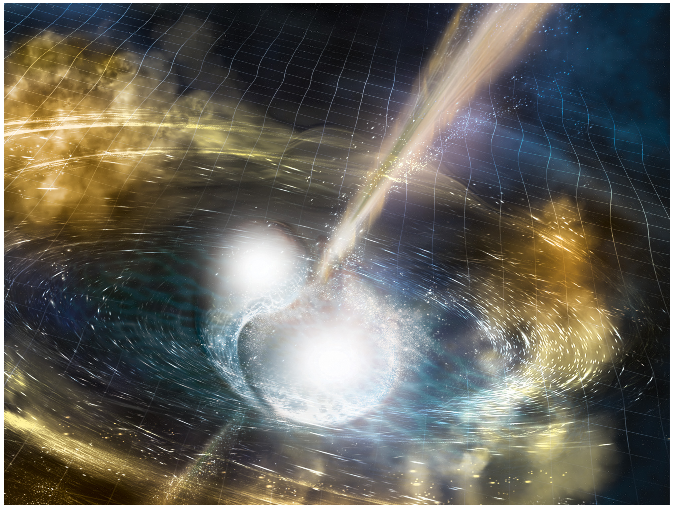

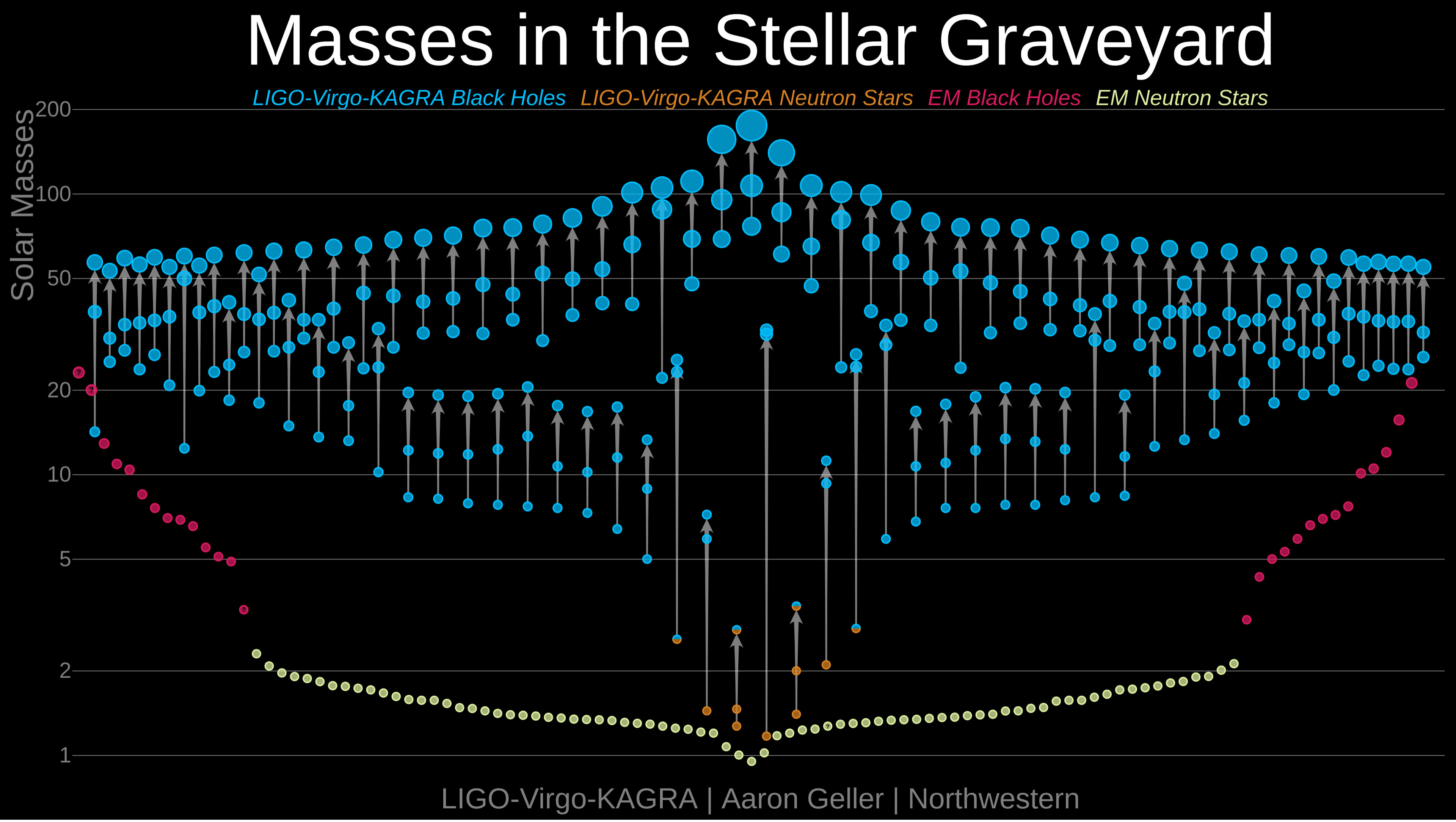

After 3 observing runs, LVK has detected 90 BBHs, 2 BNS and 2 NS-BH

During O3, detections made every few days

O4 run ongoing

What have we learned ? Some highlights:

Astrophysics

- GW170817 solved the long-standing problem of the origin of (at least some) short GRB
- NS-NS mergers are a site for the formation of some of the heaviest elements through r-process nucleosynthesis
- BH-BH binaries exist and merge within the age of the Universe
- discovered a new population of stellar-mass BHs, much heavier than those detected through X-ray binaries

Cosmology/fundamental physics

- speed of GWs equal to speed of light (1:10^{15})
- first measurement of the Hubble constant with GWs
- the tail of the waveform of GW150914 consistent with the prediction from General Relativity for the quasi-normal modes of the final BH
- deviations from GR (graviton mass, post-Newtonian coefficients, modified dispersion relations, etc.) could be tested and bounded

Still, 2G detectors lack the sensitivity to make really stringent tests of fundamental physics/cosmology

2G detectors have opened a new window

3G detectors (ET, CE) will look deeply into this window

``Qualunque sia la prospettiva da cui si osservi, fare ricerca in fisica fondamentale significa superare i limiti. Spingere, e spingersi, oltre i confini."

(dalla pagina Indico delle giornate di studio INFN)

useful references for ET

- MM et al "Science Case for the Einstein Telescope", JCAP, 1912.02622 (written for the ESFRI RoadMap)
- Iacovelli, Mancarella, Foffa, MM, ApJ, 2207.02771
- M. Branchesi, MM et al, JCAP, 2303.15923 (the "Science-CoBA" paper)
- Abac et al, ET Collaboration, 2503.12263 (the "BlueBook")
  880 pages, 200 figures, 4 yrs of work, 490 authors
  coordinated by M. Branchesi, A. Ghosh and MM

Einstein Telescope: the concept and the current situation

- single-site triangle, or 2L in different sites
- arms: 3 → 10(15) km
- 200-300 m underground
- two instruments, LF (cryogenic) and HF

ongoing studies on the best geometry and configurations

Infrastrutture di ricerca in Europa: ESFRI

Nel 2021 ESFRI ha approvato la proposta a guida del governo italiano di inserire Einstein Telescope nella roadmap delle più importanti infrastrutture di ricerca da realizzarsi nei prossimi 10 anni.
Altre 4 nazioni (NL, BE, ES, PL) hanno co-firmato la proposta.

EINSTEIN
TELESCOPE

The ET Collaboration

- Currently the ET Collaboration has > 1800 members, organized in 93 Research Units, over 264 institutions and 31 countries

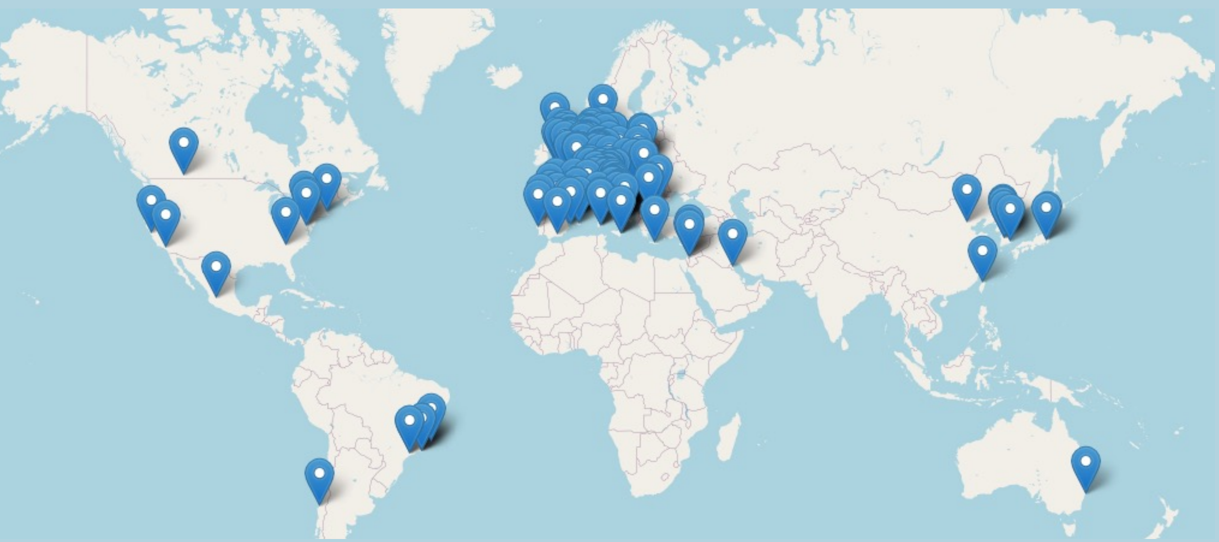

ETC organization: Specific Boards

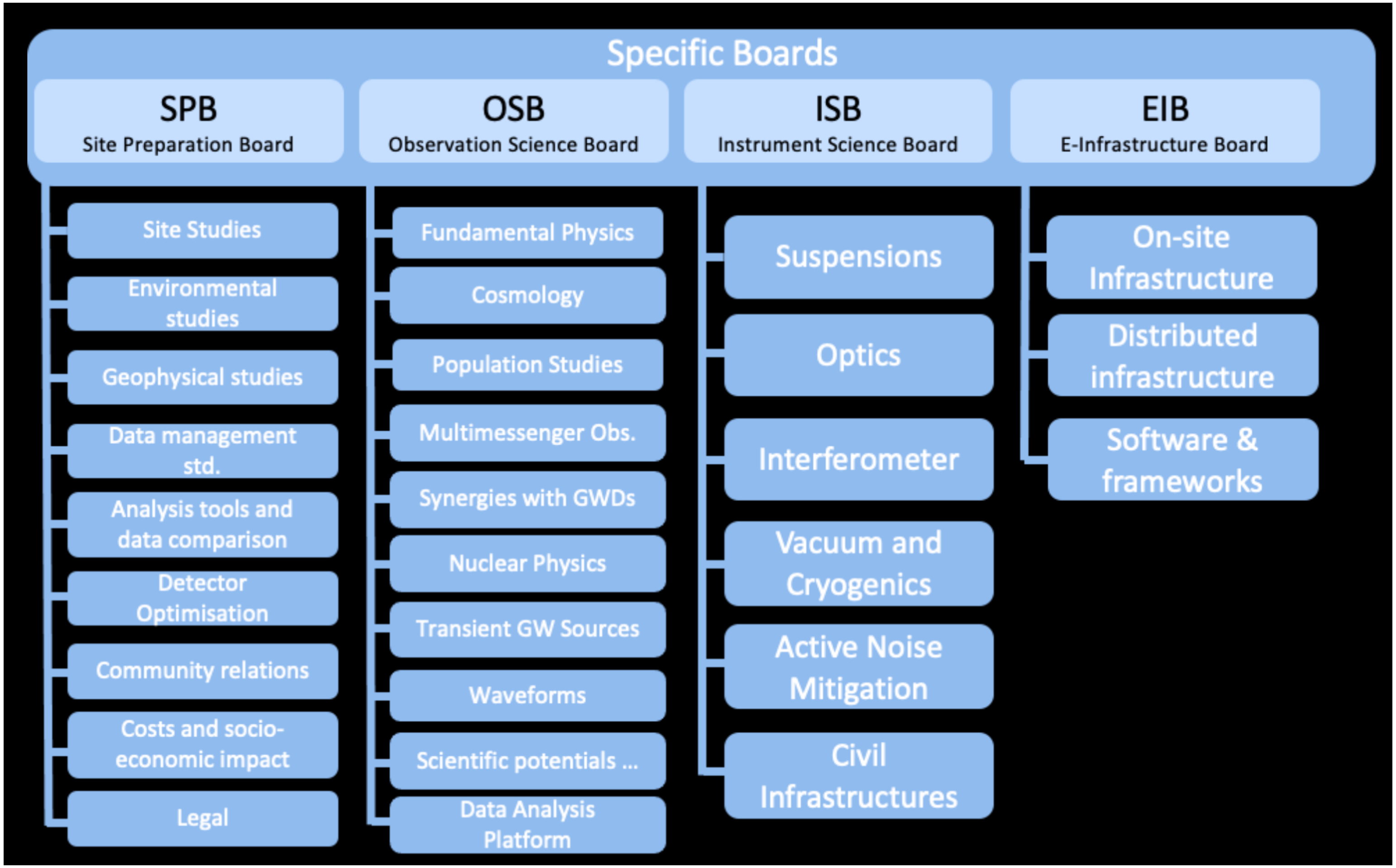

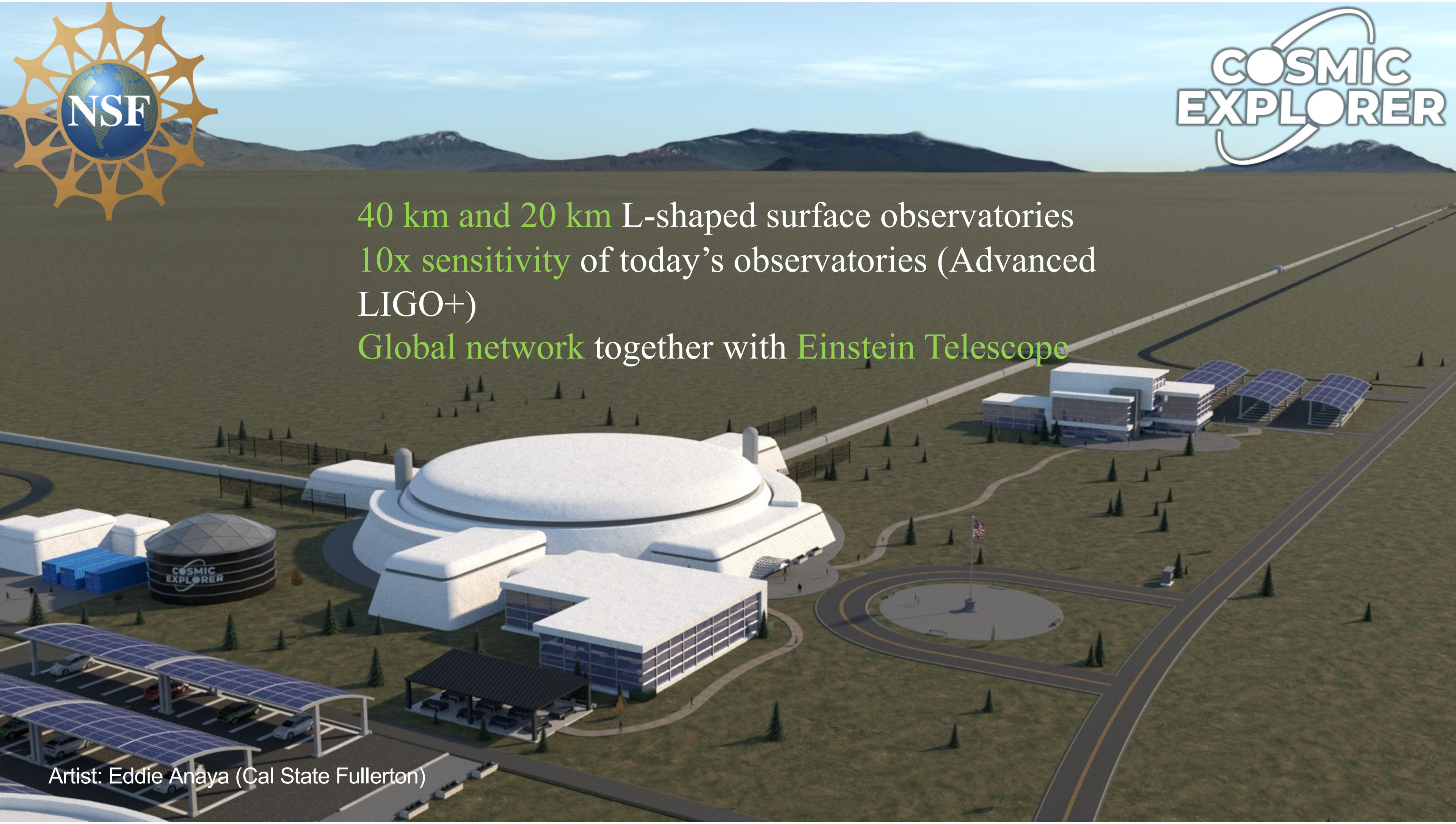
COSMIC EXPLORER
40 km and 20 km L-shaped surface observatories
10x sensitivity of today's observatories (Advanced LIGO+)
Global network together with Einstein Telescope
Artist: Eddie Anaya (Cal State Fullerton)

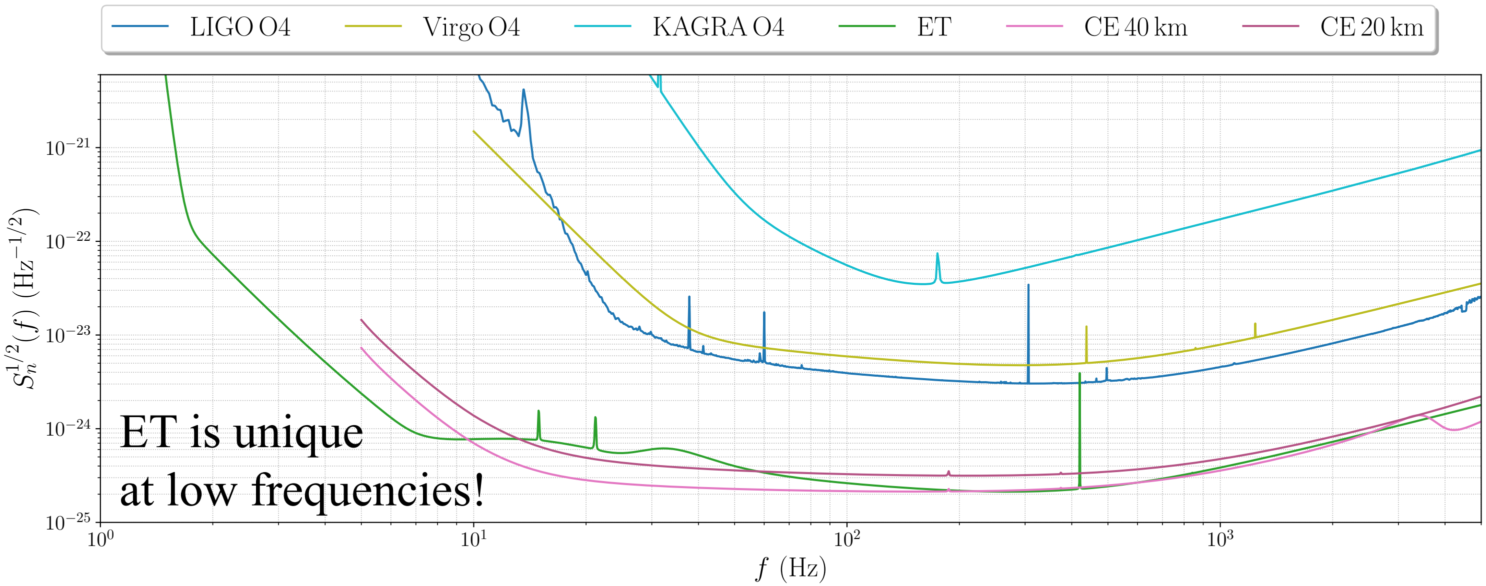

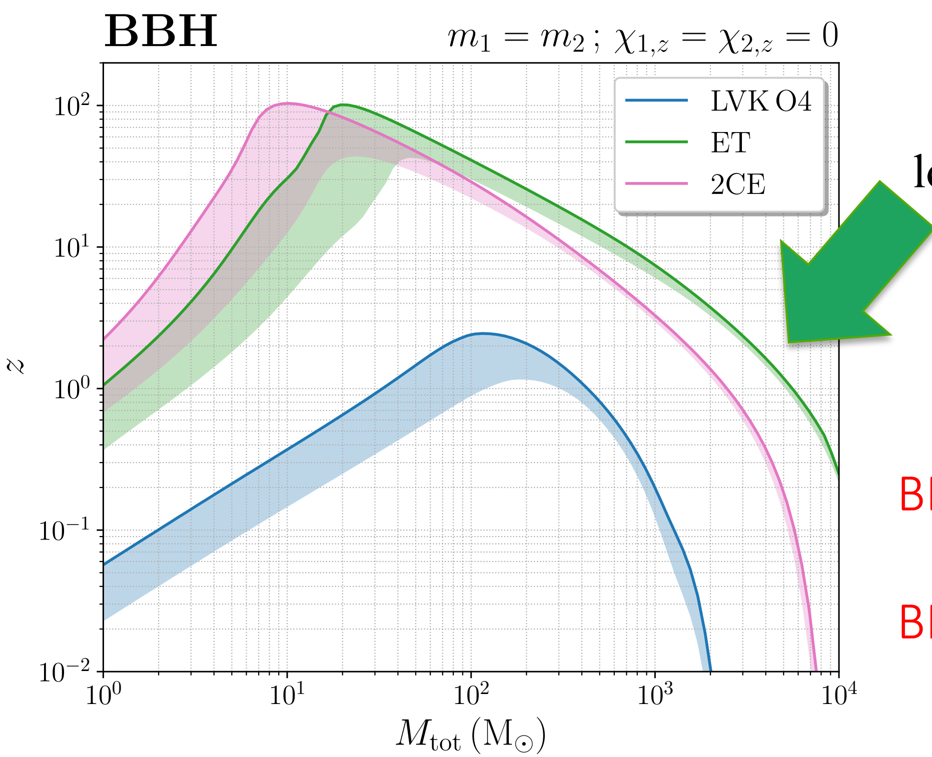

low-f sensitivity

BBH up to z=O(50-100) !!

BNS up to z ~ 3

Detection distance of BBHs

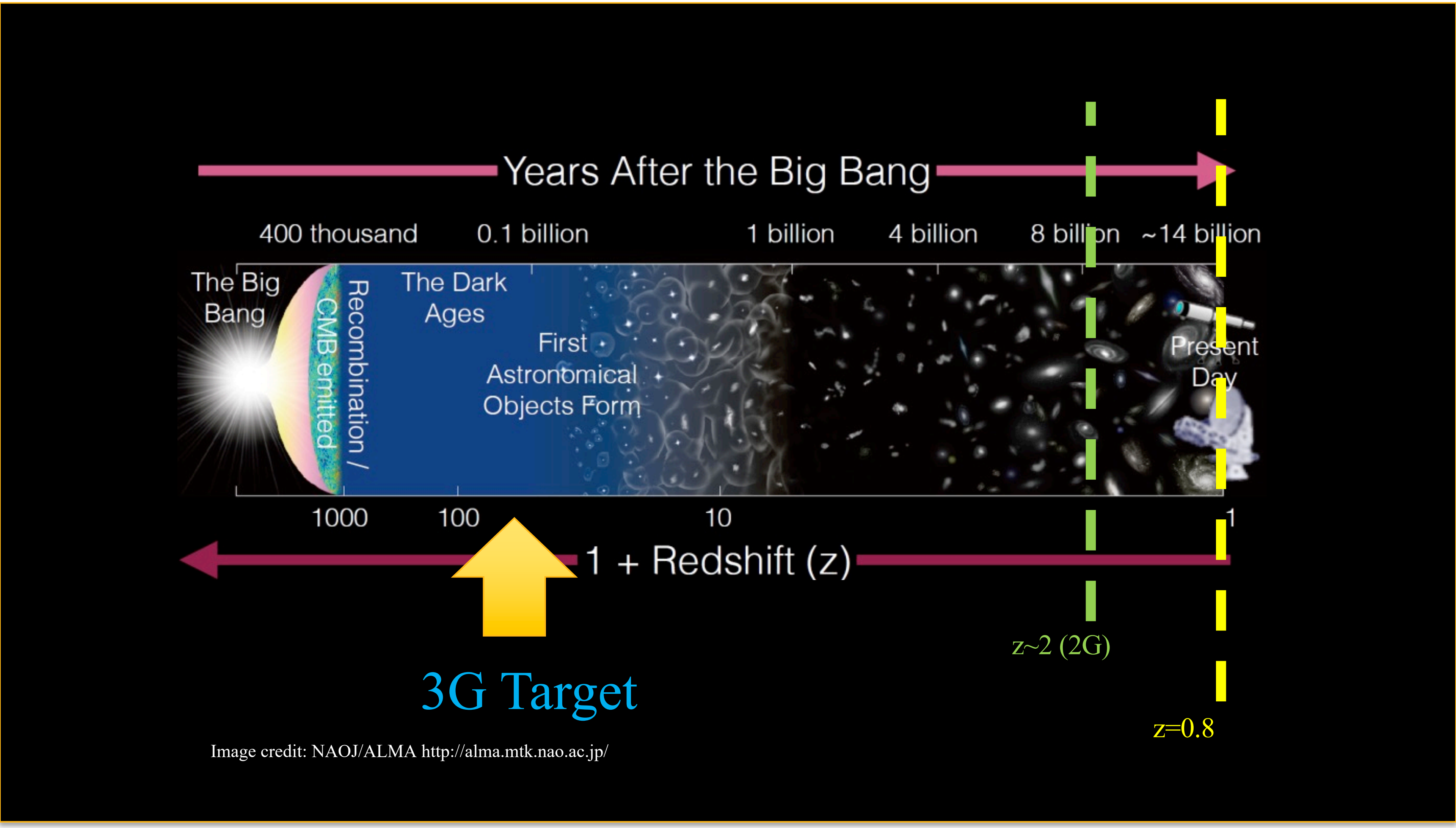

SNR distribution and examples of parameter reconstruction (BBH)

Iacovelli et al. 2022

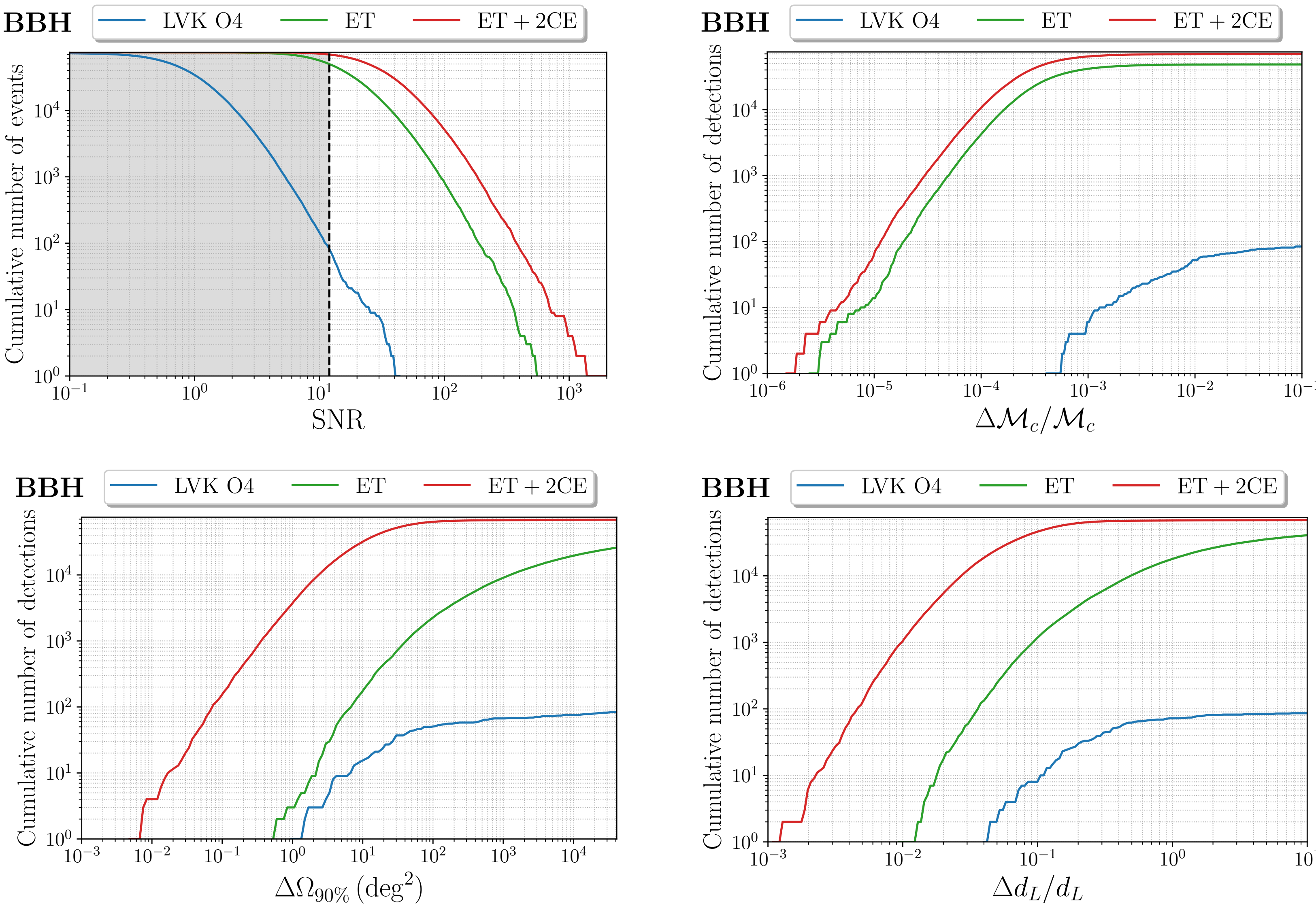

GW170817 at LVC-O2 and at ET

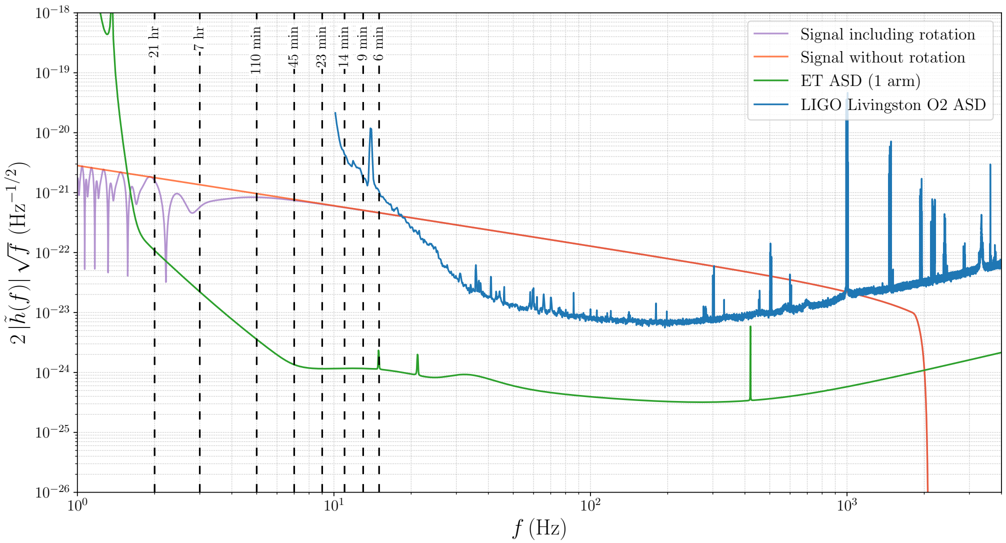

we can trigger e.m. observations before the emission of photons

Keyword: low frequency sensitivity!

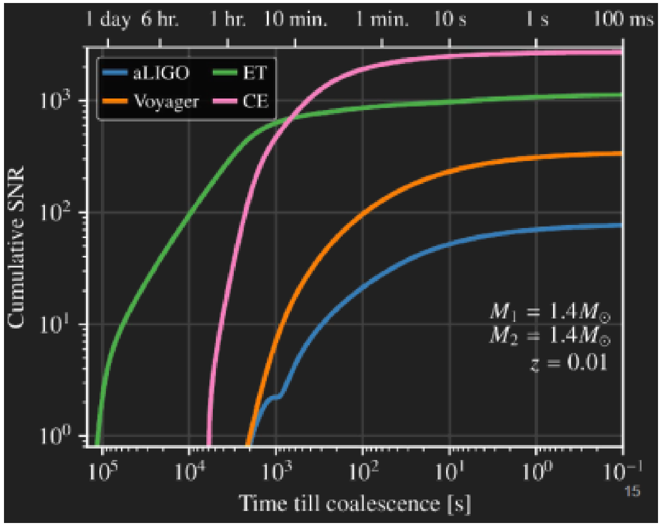

The combination of

- distances and masses explored
- number of detections
- detections with very high SNR

will provide a wealth of data that have the potential of triggering revolutions in astrophysics, cosmology and fundamental physics

see the “BlueBook” for a >800 pages description of the science case of ET

A summary of the Science of ET

Astrophysics

- Black hole properties
  - origin (stellar vs. primordial)
  - evolution, demography
- Neutron star properties
  - demography, equation of state
- Multi-messenger astronomy
  - joint GW/EM observations (GRB, kilonova,...)
  - multiband GW detection (LISA)
- Detection of new astrophysical sources
  - core collapse supernovae
  - isolated neutron stars
  - stochastic background of astrophysical origin

Fundamental physics and cosmology

- testing the nature of gravity
  - perturbative regime

    inspiral phase of BBH, post-Newtonian expansion
  - strong field regime

    physics near BH horizon

    exotic compact objects

- QCD

  interior structure of neutron stars probe:
  - QCD at ultra-high temperatures and densities
  - exotic states of matter

- Dark matter/new particles
  - primordial BHs
  - axions, dark matter accreting on compact objects

- Dark energy and modifications of gravity on cosmological scales
  - DE equation of state
  - modified GW propagation

- Stochastic backgrounds of cosmological origin and connections with high-energy physics
  - inflation
  - phase transitions
  - cosmic strings
  - ...

and we should not forget that ET will be a `discovery machine': expect the unexpected!

In the following, we elaborate just on some `selected highlights'

1. The nature of Gravity

BHs are one of the most extraordinary predictions of GR

(e.g. $10M_\odot$ concentrated in 30 km)

how can we be sure that the compact objects observed by LIGO/Virgo are the BHs predicted by GR?

- can we `quantify' the existence of horizons?
- can we test the existence of Exotic Compact Objects?

no shortage of proposals in the literature:

boson stars (self-gravitating fundamental fields)

firewalls, fuzzballs... (quantum effects near the horizon motivated by the Hawking information loss problem):

BH quasi-normal modes (QNM)

the elasticity of space-time in the regime of strong gravity!

GR predicts frequency and damping time as a function of mass and spin

classic chapter of GR: Regge-Wheeler, Chandrasekhar, Teukolsky...

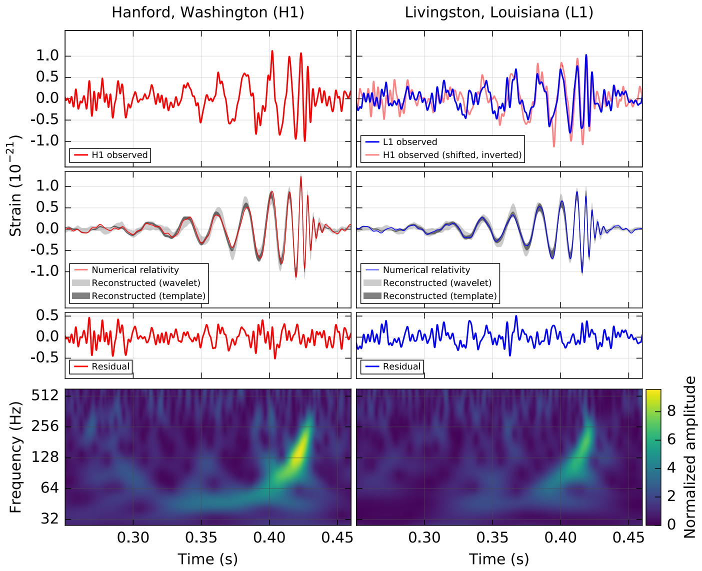

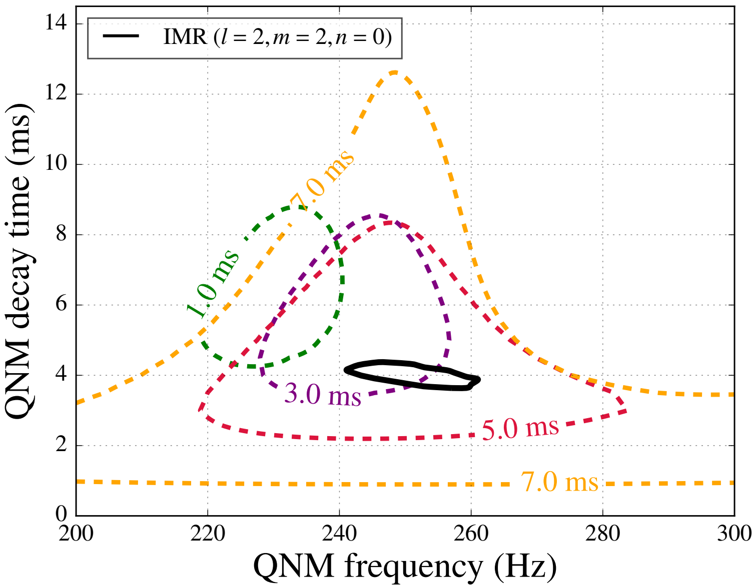

already observed in GW150914 (LVC)

consistent with GR, but we cannot say much more

BBH post-merger at ET

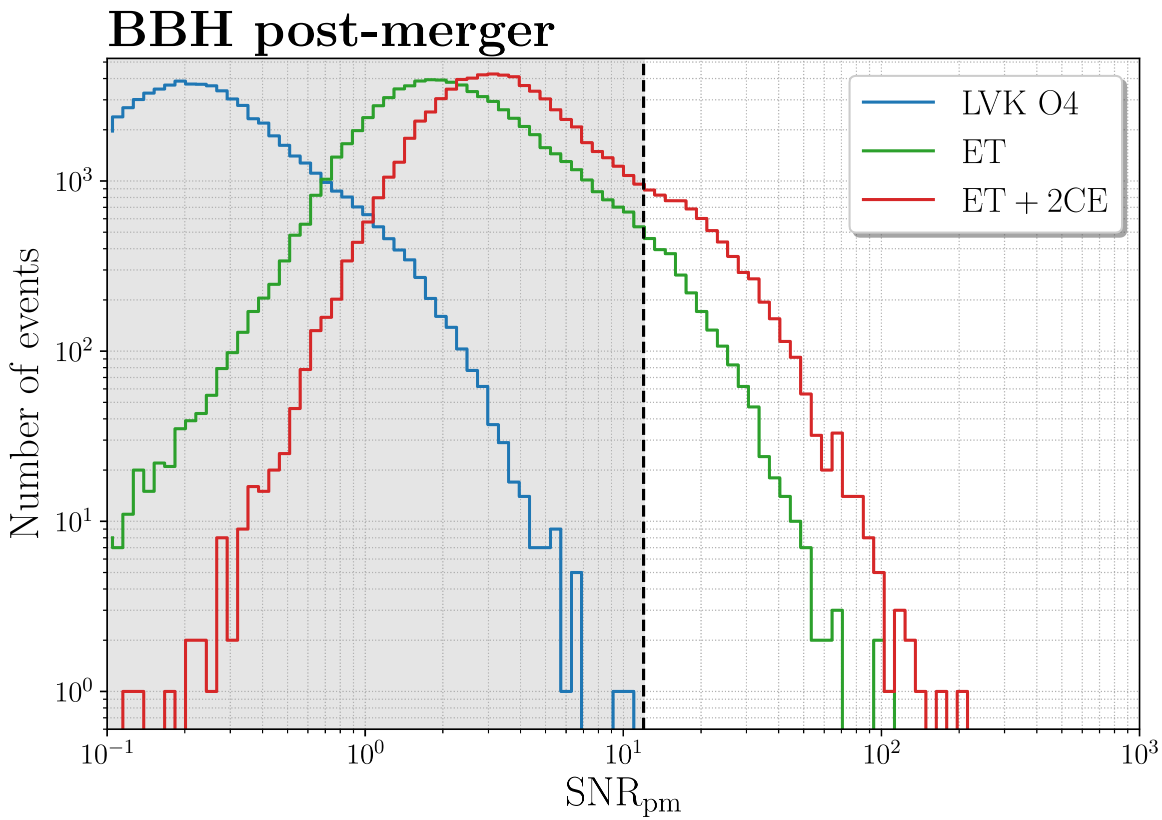

Iacovelli et al. 2022

- accurate BH spectroscopy already from single events
- 10^3 events/yr with detectable ringdown
- 20-50 events/yr with detectable higher multipoles or overtones

2. The origin of BHs: astrophysical vs primordial

ET will uncover the full population of coalescing stellar BBH since the end of the cosmological dark ages

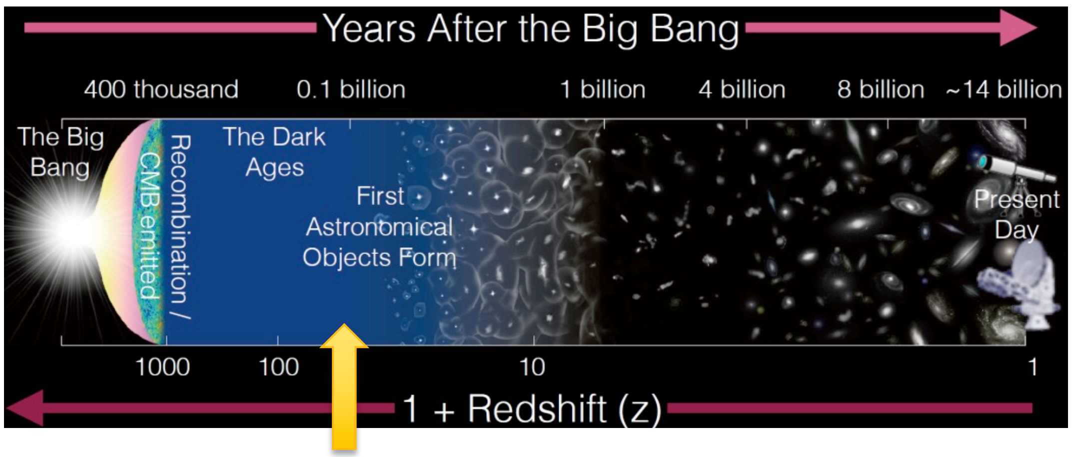

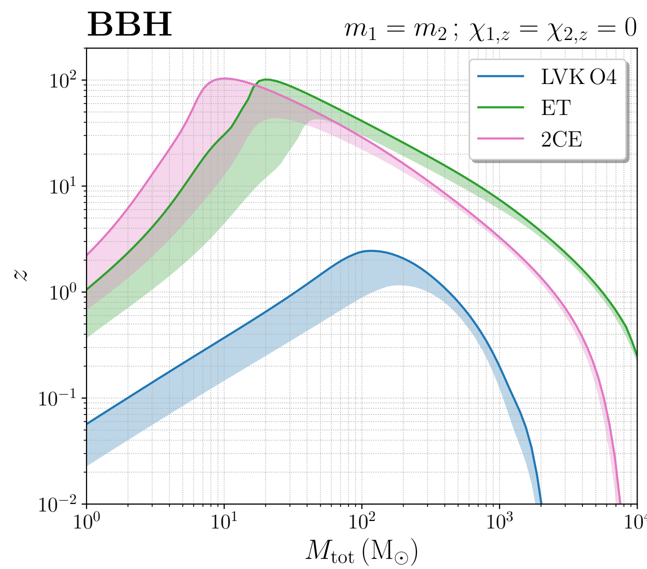

BHs can also be generated by the collapse of large over-densities in the early Universe (PBHs) → window on inflationary scales

PBHs might also contribute to dark matter

Disentangle astrophysical from primordial BH

- the PBH merger rate increases with redshift, up to z =O(10^3)

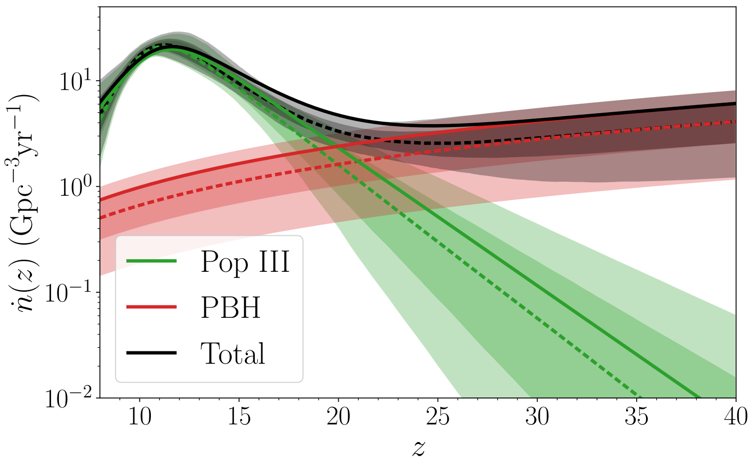

Any BBH merger at z>30 will be of primordial origin

ET can reach z~ 50-100 !!

- subsolar mass BH must be primordial

3. QCD with neutron stars

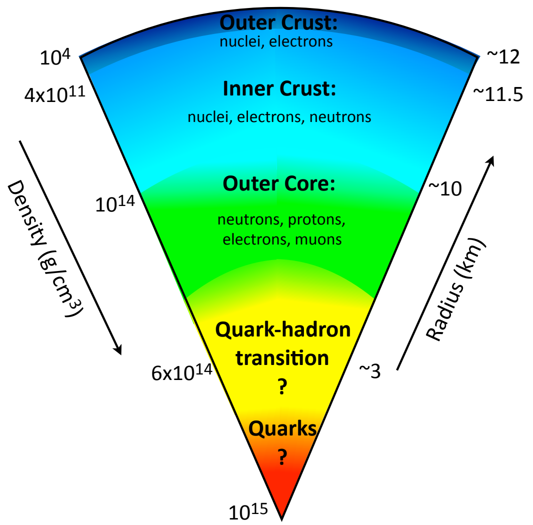

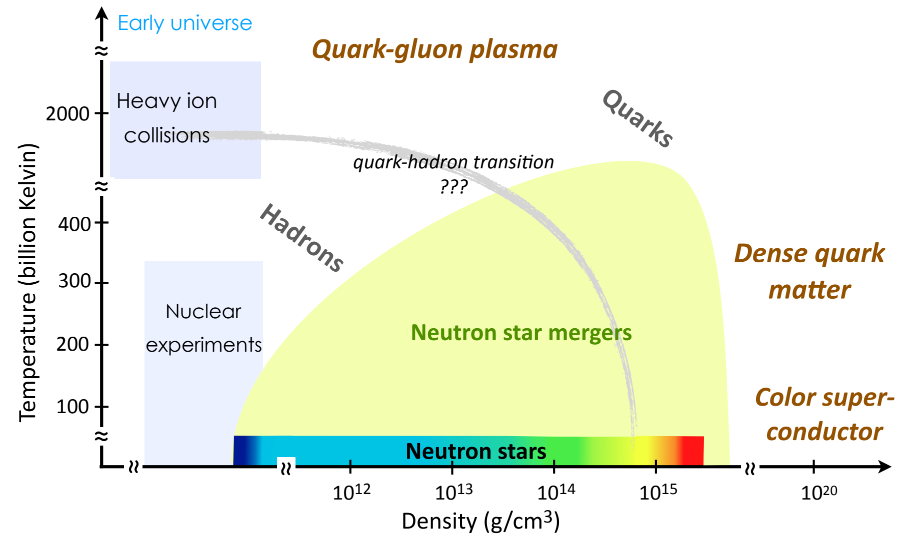

MM et al, ESFRI paper, 1912.02622

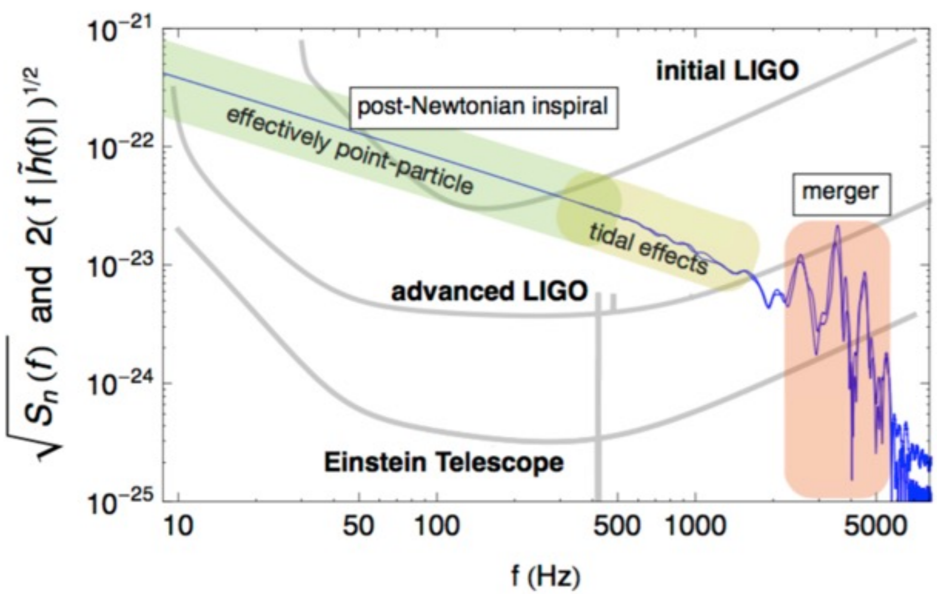

BNS merger @100 Mpc
(from J. Read)

4. Cosmology and dark energy

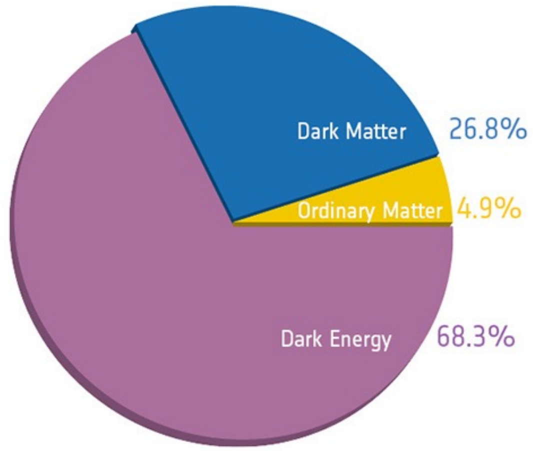

cosmology determines the relation between (luminosity) distance and redshift

$$d_L(z) = \frac{1+z}{H_0} \int_0^z \frac{d\tilde{z}}{\sqrt{\Omega_M (1+\tilde{z})^3 + \rho_{\rm DE}(\tilde{z})/\rho_0}}$$

$$\Omega_M = \frac{\rho_M(t_0)}{\rho_0}, \quad \rho_0 = \frac{3H_0^2}{8\pi G}$$

the key: the GW signal from a coalescing binary allows us to measure the distance to the source

(this is difficult with electromagnetic probes)

- low z: Hubble law, $d_L \simeq H_0^{-1} z$
- moderate z: access $\Omega_M, \rho_{\rm DE}(z)$

low z: measuring H_0

Observational tensions, in particular early- vs late-Universe probes of H_0

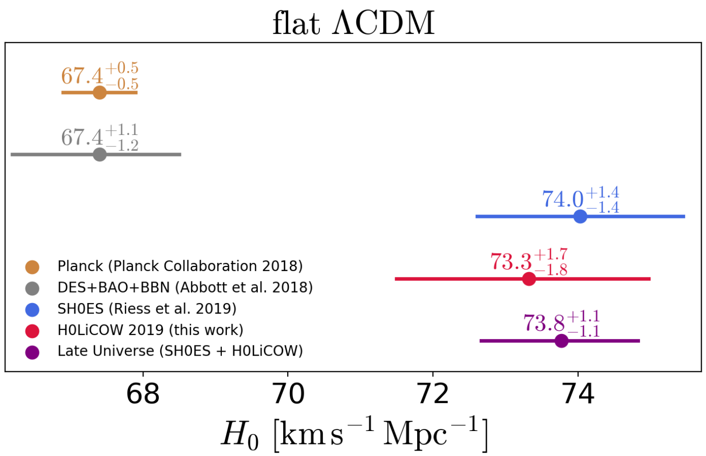

O(50-100) standard sirens at 2G needed to arbitrate the discrepancy

already solved by the time of 3G detectors? (possible, but not sure, no counterpart in O3, no BNS candidate currently in O4)

depending on the network of electromagnetic facilities at the time of ET, ET can detect several tens BNS with counterpart per year

- At higher z, accessible only to 3G detectors or LISA, we access the redshift evolution of the dark energy density

- A potentially even more interesting observable:

  modified GW propagation

Belgacem, Dirian, Foffa, MM 1712.08108 , 1805.08731
Belgacem, Dirian, Finke, Foffa, MM ,1907.02047, 2001.07619
Belgacem et al, LISA CosWG, 1907.01487

if gravity is modified at cosmologogical distances, GWs propagates differently and coalescing binaries measure a "GW luminosity distance", different from the standard (electromagnetic) luminosity distance !

$$\frac{d_L^{\rm gw}(z)}{d_L^{\rm em}(z)} = \Xi_0 + \frac{1-\Xi_0}{(1+z)^n}$$

5. Dark matter, new fundamental fields

Several DM candidates can be studied (only?) by ET

- primordial BHs
  - BBH at $z \sim 30-100$,
  - masses down to (0.1-1) $M_{\odot}$
  - correlation with Large Scale Structures

- DM particles captured in NS/BH
  - DM core in NS, drag in binary systems

Ultralight particles

particles with m ~ 10^{-20}-10^{-10} eV have Compton wavelength of order of the Schwartzschild radius of BHs with masses billions $M_\odot$ to a few $M_\odot$

10^{-22}-10^{-10} eV : lower range → viable DM candidates
upper range → QCD axions
ultralight axions from string theory possibly covering the whole range

because of a super-radiance instability, they extract energy from rotating BHs and form a long-lived Bose condensate rotating with the BH

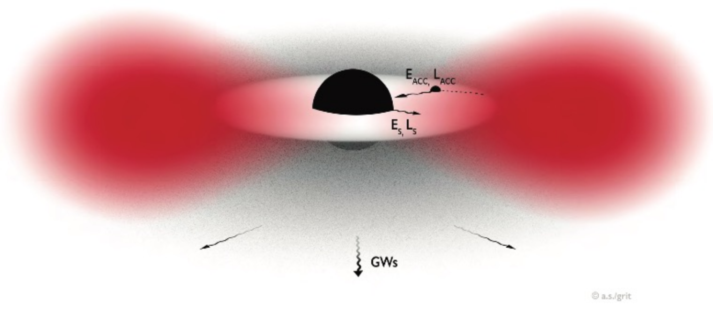

figure: Brito, Cardoso, Pani 2014

6. Stochastic GW backgrounds

GWs can carry uncorrupted information from the very earliest moments after the big bang and corresponding high-energy physics

- photons decouple from primordial plasma when

  $z \simeq 1090, \quad T \simeq 0.26$ eV

  CMB gives a snapshot of the Universe at this epoch

- neutrinos decouple at $T \simeq$ MeV

- GWs are already decoupled below the Planck scale, 10^{19} GeV

ET improves the sensitivity to stochastic backgrounds by 2-3 orders of magnitude compared to LIGO/Virgo vacuum fluctuations from slow-roll inflation too small, but other inflation-related mechanisms can produce detectable signals

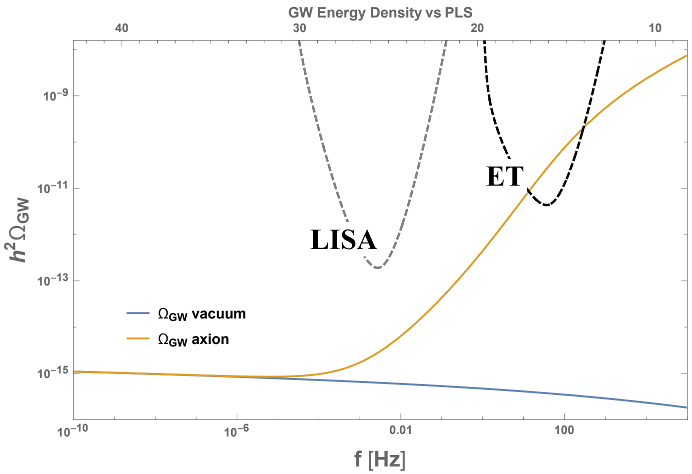

- cosmic strings
- 1^{st} order phase transitions at T $\sim 10^7$-10^{10} GeV
- anisotropies, multipole expansion

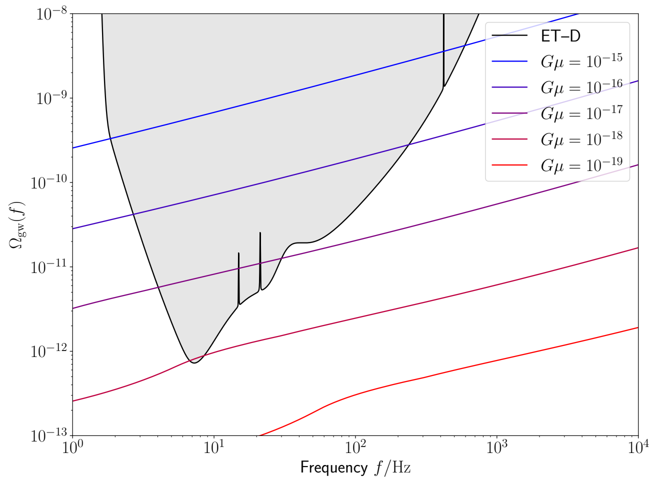

Take-away messages

ET has an exciting and broad science program, ranging from astrophysics to cosmology and fundamental physical

Thank you!

bkup slides

The Science Case of ET is very broad

a “teaser”: a glimpse from the table of content of the BlueBook chapters

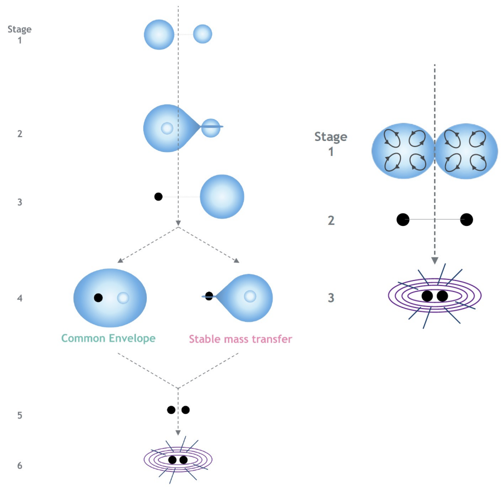

Figure 3.1: Evolutionary pathways to form a GW source for isolated binary evolution. Left: the common-envelope channel and the stable mass transfer channel. Stage 1) Zero-Age-Main-Sequence (ZAMS) 2) First phase of mass transfer 3) Formation of BH or NS 4) Second phase of mass transfer 5) Formation of double compact object 6) GW merger. Right: chemically homogeneous evolution. Stage 1) ZAMS 2) Formation of binary BH 3) GW merger.

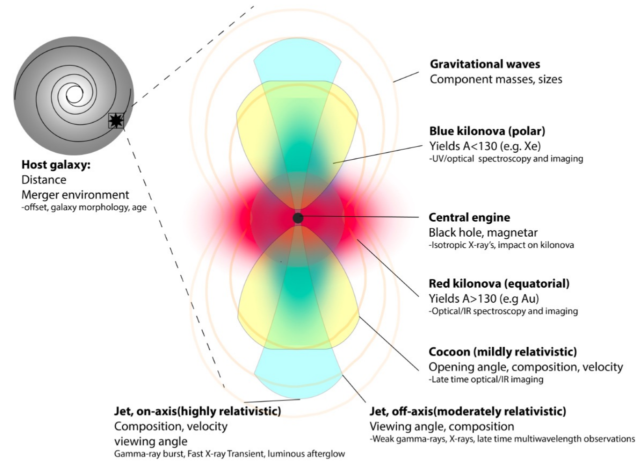

Figure 4.2: The physical process ongoing in the merger of a binary system of neutron stars (or a neutron star and a black hole), their multi-messenger observational signals and the scientific insight enabled from them (updated from an original concept by [2173]). Gravitational wave observations provide robust measurement of the component masses, and constraints on their sizes and spins. Many possible electromagnetic signals are also possible, including the detection of associated GRBs, cocoon emission, and kilonova signatures.

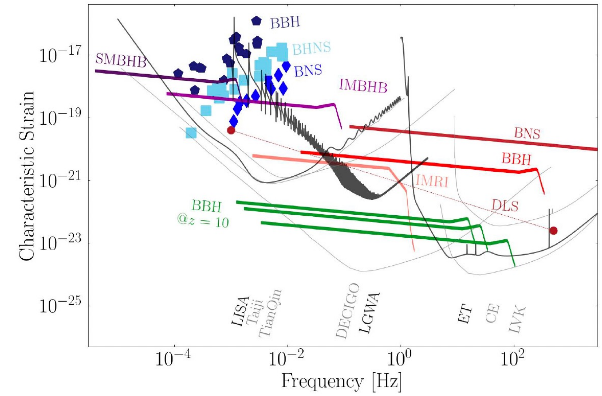

BBH
BHNS
BNS
SMBHB
IMBHB
BNS
BBH
IMRI
DLS
BBH
@z = 10
LISA
Taiji
TianQin
DECIGO
LGWA
ET
CE
LVK
Characteristic Strain
Frequency [Hz]

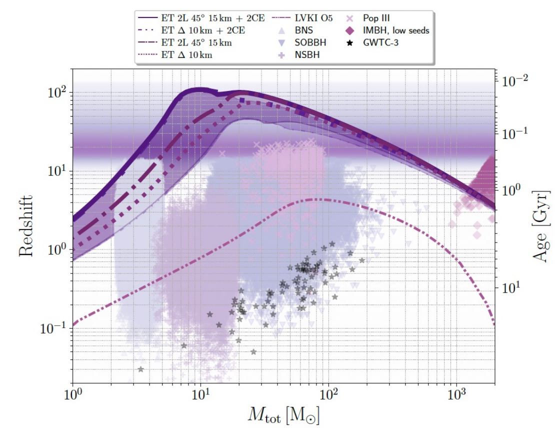

ET 2L 45° 15 km + 2CE
ET Δ 10 km + 2CE
ET 2L 45° 15 km
ET Δ 10 km
LVKI O5
BNS
SOBBH
NSBH
Pop III
IMBH, low seeds
GWTC-3
Redshift
Age [Gyr]
$M_{\rm tot}$ [$M_\odot$]

SN explosion driven by QCD phase transition

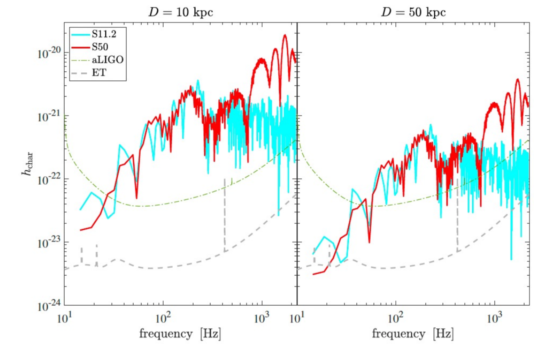

Figure 6.14: Characteristic GW spectral amplitudes, $h_{\rm char}$, for the two models S11.2 (light blue solid lines) and S50 (red solid lines) shown in figure 6.13, assuming a source distance of 10 kpc (left panel) and 50 kpc (right panel). The noise amplitudes of aLIGO (green dashed lines) and ET (grey dashed lines) are plotted as references. Figure reproduced based on data from ref. [3019].

post-merger signals and EoS

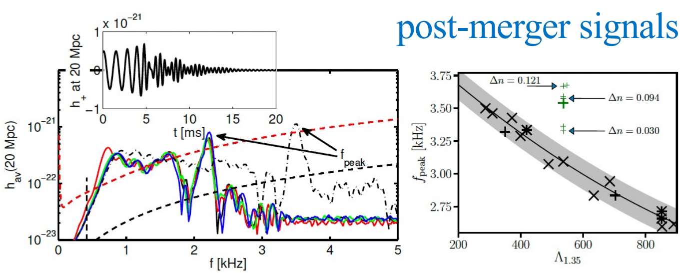

Figure 6.9: Left panel: Orientation-averaged spectra of the GW signal for different EOSs and the Adv LIGO (red dashed) and ET (black dashed) sensitivity curves. The inset shows the GW amplitude of the + polarization at a distance of 20 Mpc for one of the EOSs. Figure from ref. [2932]. Right panel: Peak frequency of the postmerger GW emission as a function of tidal deformability Λ for a $1.35M_\odot - 1.35M_\odot$ NS-NS merger. Black symbols are for purely

EoS constraints from multi-messenger observations

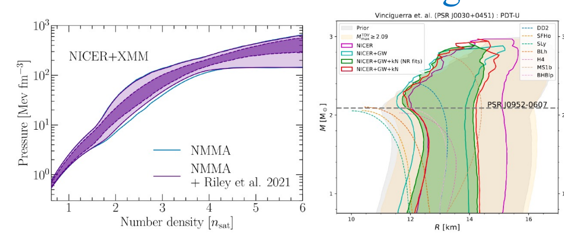

Figure 6.18: Examples of constraints on the nuclear EOS obtained by joint multimessenger analysis combining astrophysical observations of pulsars, NICER measurements, GW170817 and GW190425, kilonova AT2017gfo and GRB170817A modeling. Left: Posteriors for the pressure as a function of number density with (purple) and without (blue) NICER and XMM observations of PSR J0740+6620. Right: Posteriors in the M-R diagram of the GW-only (blue), joint (red), and NR-informed joint analysis (green). Figures adapted from [3132] (left) and [3138] (right).

SNR for SNe with different progenitors

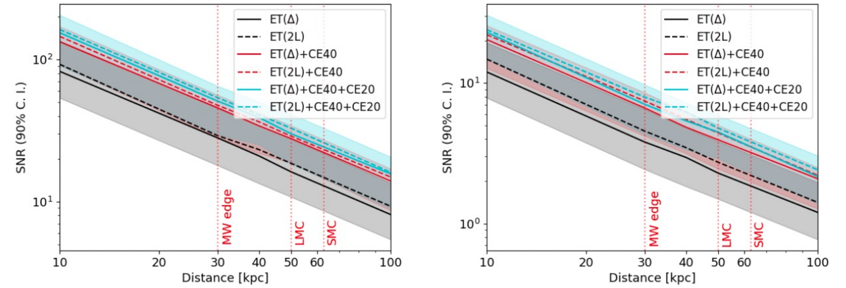

Figure 7.16: Expected SNR as a function of distance for the 15.01 (top plot) and 9a (bottom plot) models corresponding to a progenitor mass of 15.01 $M_\odot$ and 9 $M_\odot$ [2991], respectively.

core-collapse SN, PSN oscillations

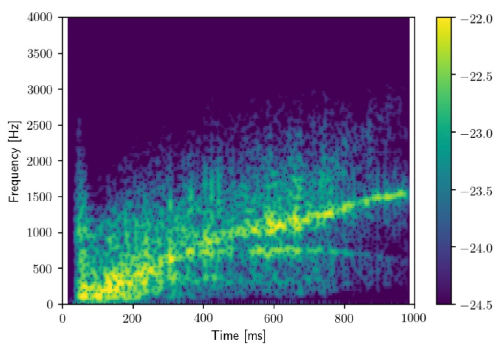

Figure 7.8: Spectrogram of a typical core-collapse simulation showing the tracks of different oscillation modes of the PNS [2997].

GWs from f-mode excitation by pulsar glitches

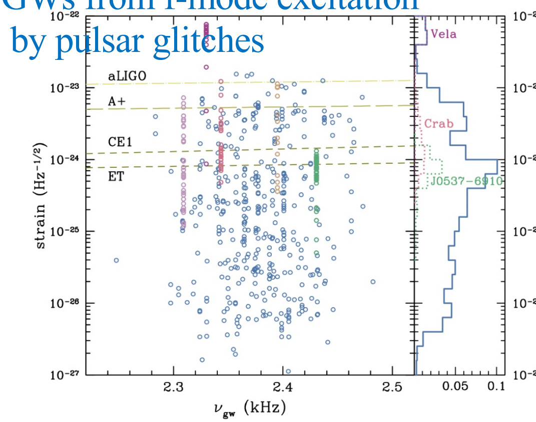

Figure 7.17: Each circle represents a value of $h_0\sqrt{\tau_{GW}}$ for f-modes excited by glitches of different pulsars and the sensitivity of several GW detectors are plotted as horizontal dashed lines. Points that lie above the sensitivity curve have signal-to-noise ratio estimates greater than 1. Typically, one would require a signal-to-noise greater than ∼10 before a detection is

continuous waves

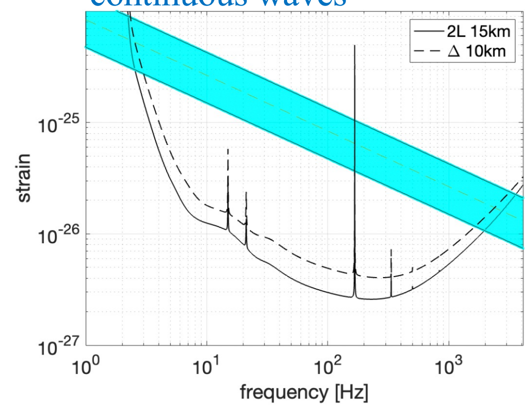

Figure 7.18: Estimated ET sensitivity (solid line: 2L 15 km configuration, dashed line: triangular 10 km configuration - 1 year of data, duty cycle 85%, drift time of 10 days) to CW emission from Sco-X1 using the semi-coherent Viterbi algorithm [3651]. The transversal orange dashed line represents the standard torque balance limit (with an average over the star rotation axis inclination), assuming surface accretion. The cyan band indicates torque balance strains from circular polarization (lower) to linear polarization (upper).

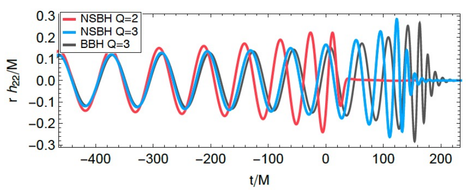

Figure 8.5: *Features of NSBH waveforms* from the SXS catalog [3836] for nonspinning systems, which were aligned at early times. The case with mass ratio $Q = 2$ (red curve) clearly shows the shutoff due to tidal disruption. For $Q = 3$, the NSBH waveform (blue curve) is similar to the corresponding BBH case (dark grey curve) up to a small dephasing due to tidal effects and details in the evolution near the plunge-merger (not visible on this

NSBH: plunge or tidal disruption

hyperbolic BBH encounters

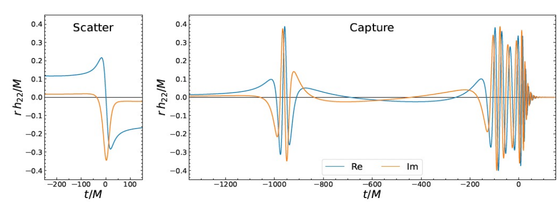

Figure 8.2: Exemplary waveforms of hyperbolic BBH encounters where the two BHs are initially unbound. The left panel shows a scattering event where the BHs remain unbound,

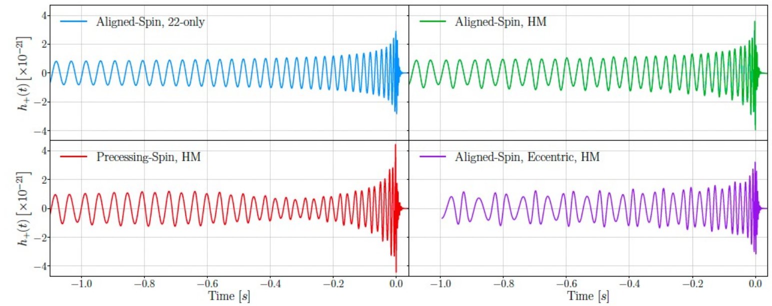

Figure 8.3: Exemplary IMR waveforms of coalescing binary black holes with mass ratio 1 : 3 and a total source-frame mass of $60 M_\odot$ located at a distance of 100 Mpc and viewed under an inclination angle of $\pi/3$ relative to the line-of-sight. The initial GW frequency is

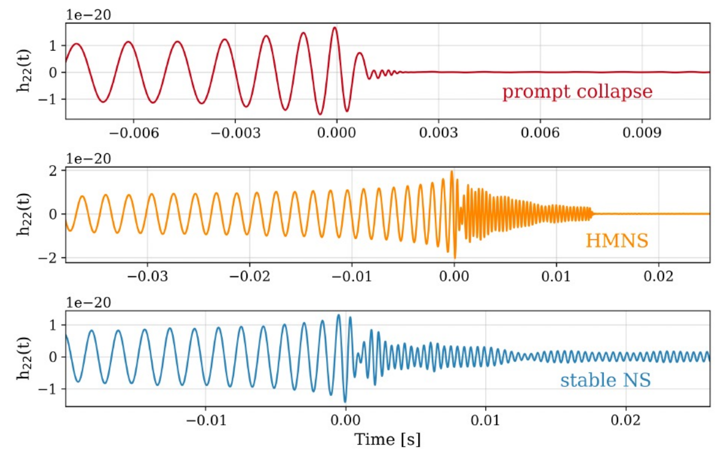

Figure 8.4: Selection of binary neutron star waveforms from NR simulations showcasing three different postmerger phenomenologies: The top panel shows prompt collapse to a black hole; the middle panel shows the formation of a hypermassive neutron star (HMNS), and the bottom panel shows the formation of a stable neutron star. The simulations are BAM:0005 [4448], THC:0084 [3091] and BAM:0080 [2386], publicly available from the CoRE database [2258].

	GWBench	GWFast	GWFish	TiDoFM	GWJulia
link	GWBench	CosmoStatGW/gwfast	GWFish	TiDoFM	GWJulia
domain	Frequency	Frequency	Frequency	Time	Frequency
language	`Python`	`Python`	`Python`	`Python`	`Julia`
waveforms	`LALSimulation`	self+`LALSimulation`	`LALSimulation`+num.	`Pycbc`	self
derivatives	an.+fd.	an.+AD or +fd.	an.+fd.	num.	AD
inversion	`mpmath`	Cho.,LU,SVD+`mpmath`	SVD		Cho.
reference	[4633]	[2275]	[256]	[4634, 4635]	[4636]

Table 9.1: Summary of main characteristics of the five Fisher matrix codes. Abbreviations used are: an. for analitical, fd. for finite differences method, num. for numerical, AD for automatic differentiation, Cho. for Cholesky. See text for other pipeline–specific features.

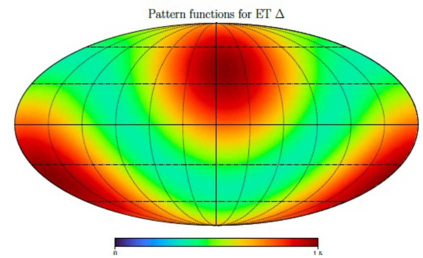

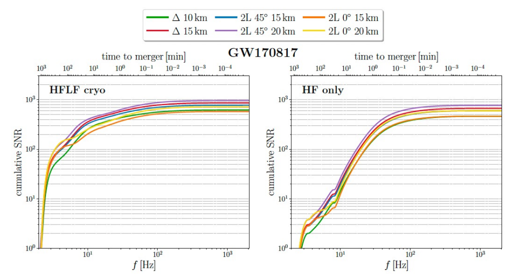

Figure 9.10: Cumulative SNR for a system with the maximum likelihood parameters of GW170817, observed by different ET configurations, as a function of GW frequency. The corresponding time to merger is shown in the upper horizontal axis. Left panel: using the ET sensitivity curve which includes both the HF and the LF interferometers, with the latter at cryogenic temperatures. Right panel: using only the the HF interferometer.

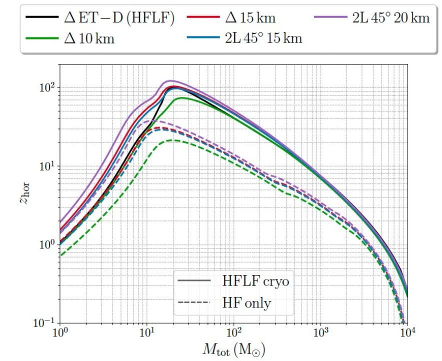

e 9.8: Detection horizons for equal–mass non–spinning binaries as a function of the –frame total mass for different ET configurations.

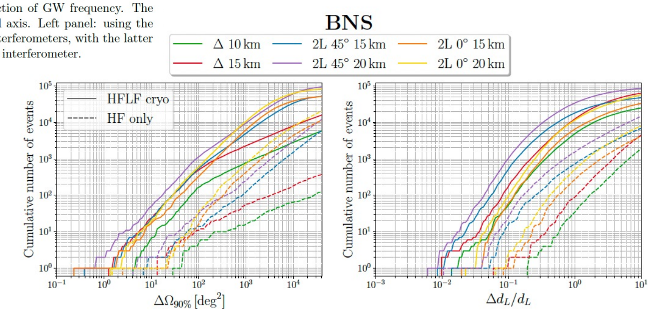

Figure 9.13: Cumulative distributions of the accuracy on angular localization (left panel) and luminosity distance (right panel) for BNSs observed by ET in the different configurations studied in [16].

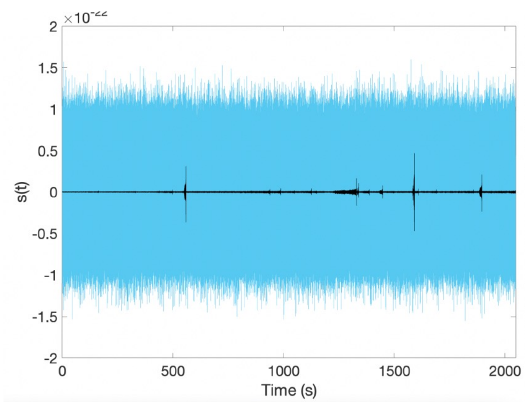

first MDC data

effect of overlapping signals on posteriors

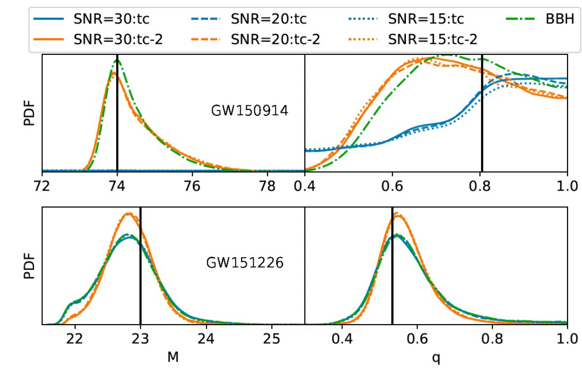

Figure 10.2: Posterior PDFs for total mass and mass ratio, for the GW150914-like signal (top panel) and the GW151226-like signal (bottom panel) when they are respectively being overlapped with a BNS signal with SNR = 30 (solid lines), SNR = 20 (dashed lines), and SNR = 15 (dotted lines). The overlaps are made so that the BBH and the BNS end at the

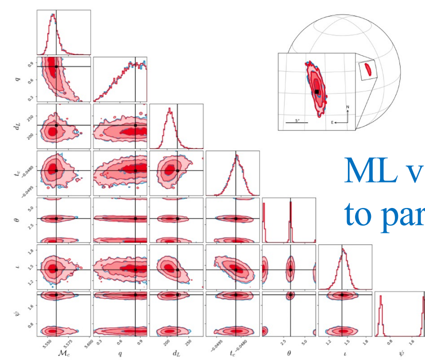

ML vs standard approach to parameter estimation

Figure 10.4: Representation of the posteriors obtained with the approach from [4799] (red) and the posteriors obtained with traditional approaches (blue) for a system with a chirp mass of $5\,M_\odot$ injected in an LVK network. A good agreement is obtained between the two posteriors, which required an adapted training procedure due to the relatively low mass of the system. To obtain this agreement, the priors during the training process have been adapted to have an effectively uniform coverage of the mass parameter space.

`golden events'

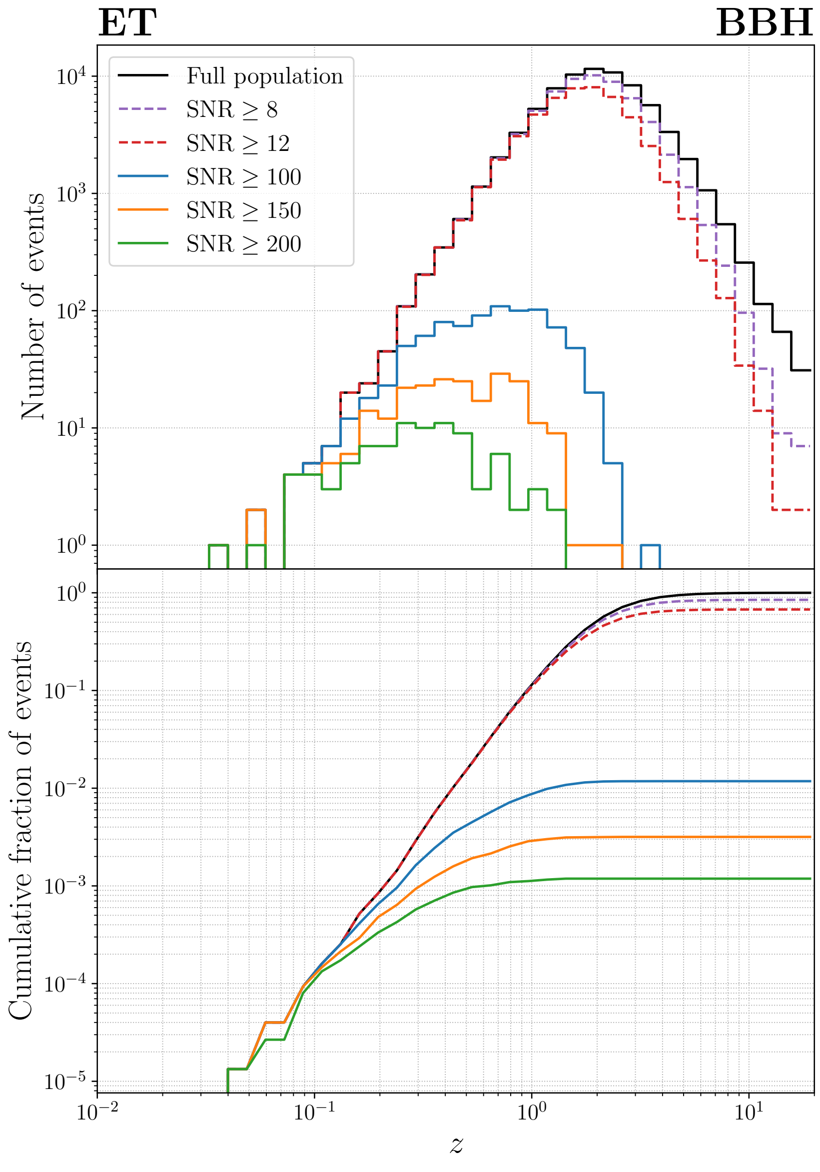

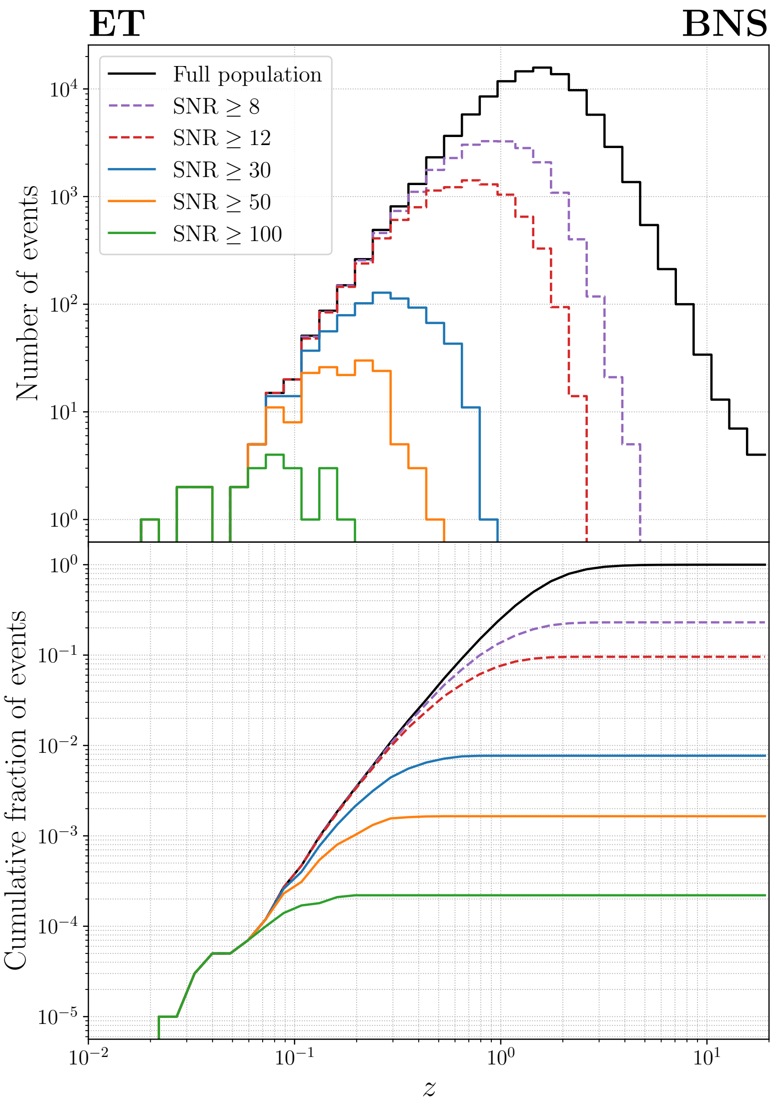

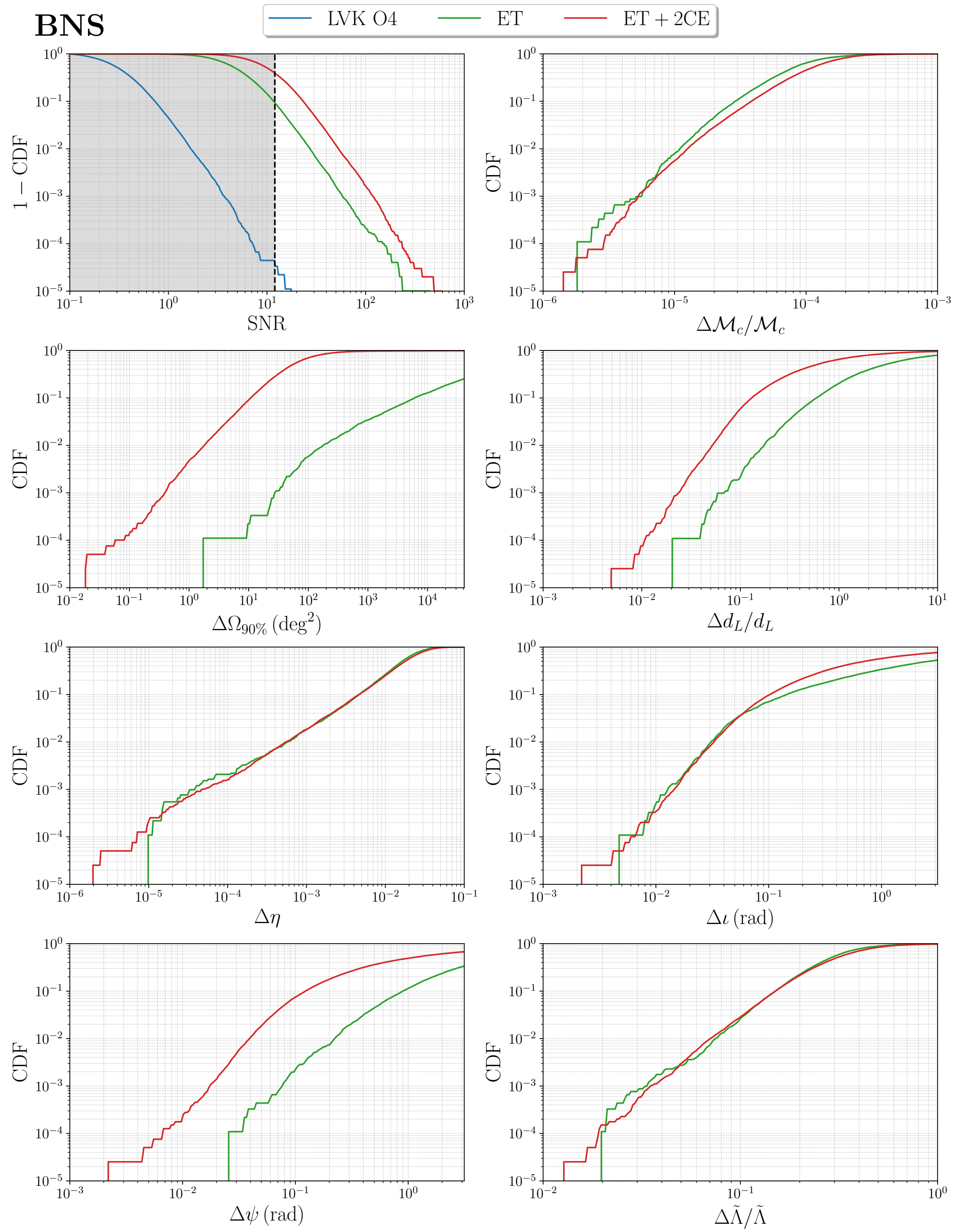

BNS
LVK O4
ET
ET + 2CE
1 − CDF
SNR
CDF
$\Delta\mathcal{M}_c/\mathcal{M}_c$
$\Delta\Omega_{90\%}\,(\mathrm{deg}^2)$
$\Delta d_L/d_L$
$\Delta\eta$
$\Delta\iota$ (rad)
$\Delta\psi$ (rad)
$\Delta\tilde{\Lambda}/\tilde{\Lambda}$

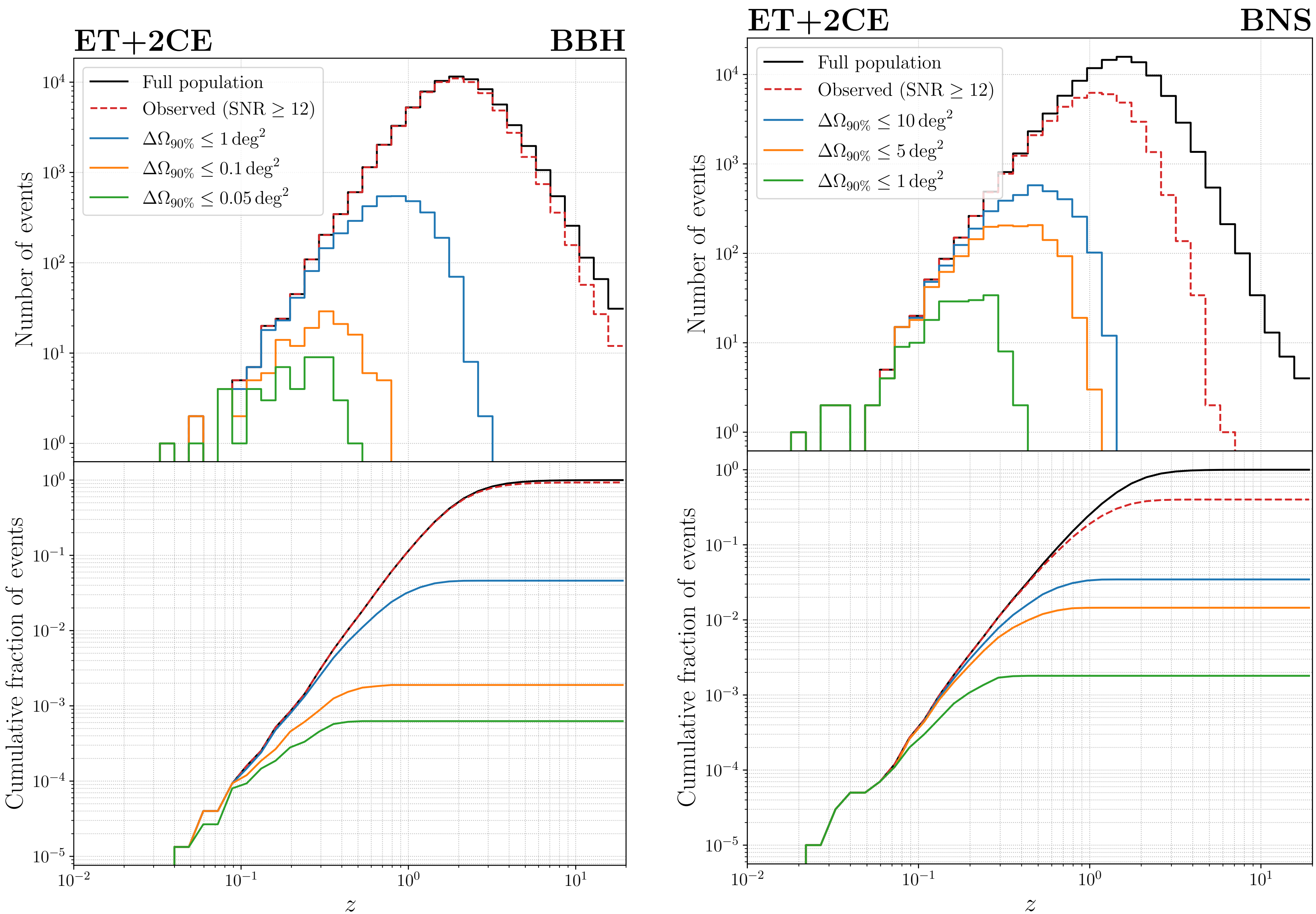

ET+2CE
BBH
Full population
Observed (SNR ≥ 12)
$\Delta\Omega_{90\%} \leq 1\,\mathrm{deg}^2$
$\Delta\Omega_{90\%} \leq 0.1\,\mathrm{deg}^2$
$\Delta\Omega_{90\%} \leq 0.05\,\mathrm{deg}^2$
Number of events
Cumulative fraction of events
z
ET+2CE
BNS
Full population
Observed (SNR ≥ 12)
$\Delta\Omega_{90\%} \leq 10\,\mathrm{deg}^2$
$\Delta\Omega_{90\%} \leq 5\,\mathrm{deg}^2$
$\Delta\Omega_{90\%} \leq 1\,\mathrm{deg}^2$
Number of events
Cumulative fraction of events
z

Modified GW propagation

in GR : $$\tilde{h}''_A + 2\mathcal{H}\tilde{h}'_A + k^2\tilde{h}_A = 0$$

$$\tilde{h}_A(\eta, \mathbf{k}) = \frac{1}{a(\eta)}\tilde{\chi}_A(\eta, \mathbf{k})$$

$$\tilde{\chi}''_A + \left(k^2 - a''/a\right)\tilde{\chi}_A = 0$$

inside the horizon $a''/a \ll k^2$, so $\tilde{\chi}''_A + k^2\tilde{\chi}_A = 0$

1. GWs propagate at the speed of light

2. $h_A \propto 1/a$ For coalescing binaries this gives $h_A \propto 1/d_L(z)$

In several modified gravity models:

$$\tilde{h}''_A + 2\mathcal{H}[1-\delta(\eta)]\tilde{h}'_A + k^2\tilde{h}_A = 0$$

$$\tilde{h}_A(\eta,\mathbf{k}) = \frac{1}{\tilde{a}(\eta)}\tilde{\chi}_A(\eta,\mathbf{k}) \qquad \frac{\tilde{a}'}{\tilde{a}} = \mathcal{H}[1-\delta(\eta)]$$

$$\tilde{\chi}''_A + (k^2 - \tilde{a}''/\tilde{a})\tilde{\chi}_A = 0 \qquad \tilde{a}''/\tilde{a} \ll k^2$$

1. $c_{GW} = c$ ok with GW170817 (otherwise the model is ruled out)

2. $\tilde{h}_A \propto 1/\tilde{a}$

All dynamical theories of DE will display this effect!

(Belgacem et al., LISA CosmoWG, JCAP 2019) coalescing binaries measure a ``GW luminosity distance" different from the standard (electromagnetic) luminosity distance !

in terms of δ(z) :

$$d_L^{\rm gw}(z) = d_L^{\rm em}(z) \exp\left\{ - \int_0^z \frac{dz'}{1+z'}\, \delta(z') \right\}$$

a general parametrization of modified GW propagation

$$\frac{d_L^{\rm gw}(z)}{d_L^{\rm em}(z)} = \Xi_0 + \frac{1-\Xi_0}{(1+z)^n}$$

Belgacem, Dirian, Foffa, MM
PRD 2018, 1805.08731

This parametrization is very natural, and fits the result of (almost) all modified gravity models

Belgacem et al (LISA CosmoWG), 2019

- for scalar perturbations, deviations from GR are bounded at the level (5-10)%

- one would expect similar deviations in the tensor sector. Instead, in a viable model (non-local gravity) the deviations at the redshifts explored by ET can reach 80% !

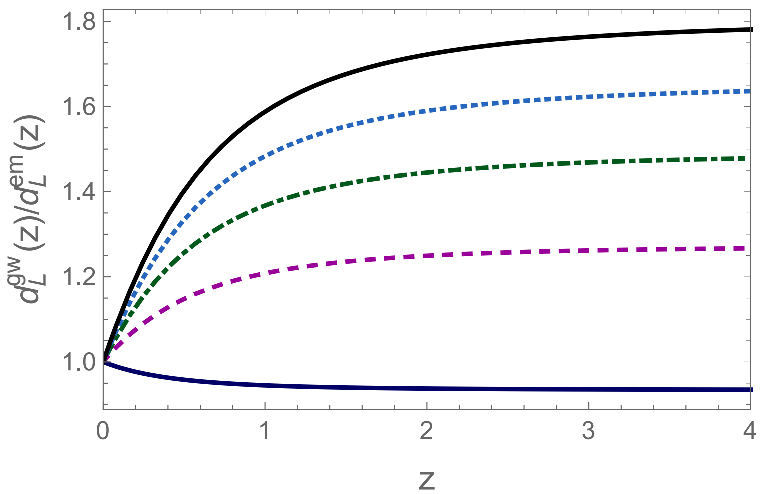

Belgacem, Dirian, Finke, Foffa, MM , 2020

⟹ 3G detectors could be the best experiments for studying dark energy

"Dark sirens": cosmology with the BNS mass function at ET

GW detectors measure the combination $m_{\rm det} = (1+z)m$
and do not measure directly z but d_L $\Longrightarrow$ here cosmology enters

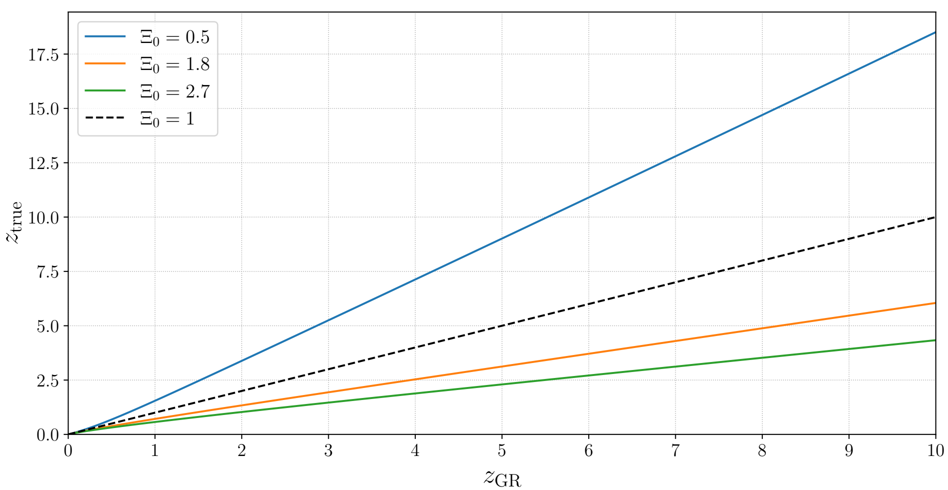

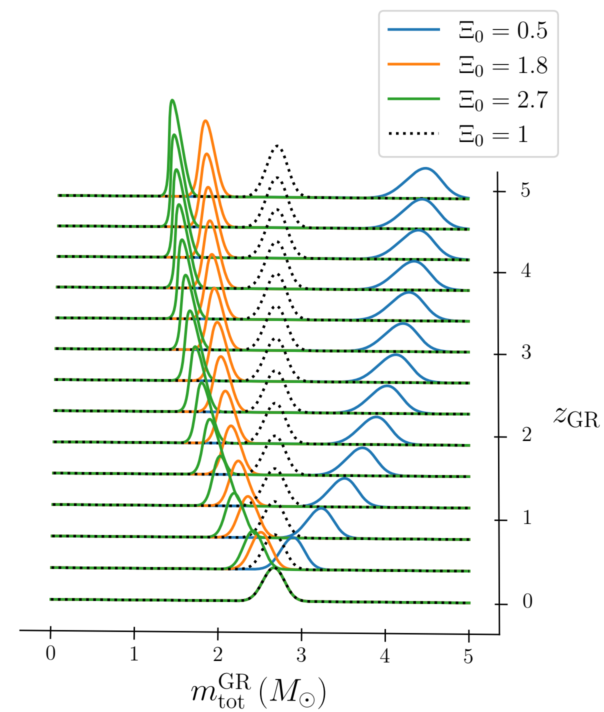

Finke, Foffa, Iacovelli, MM, Mancarella 2021

Echoes from Exotic Compact Object

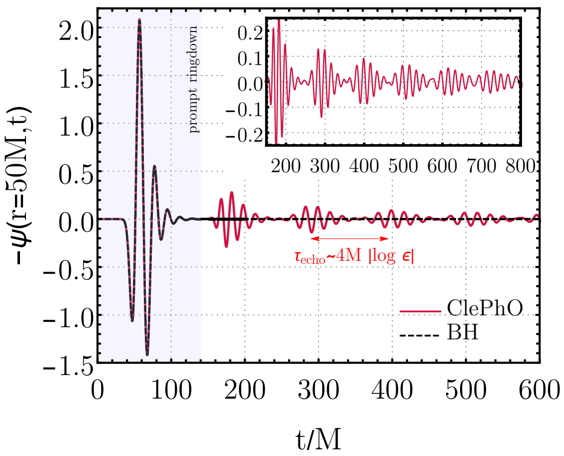

Cardoso, Franzin, Pani 2016

$$\tau_{\rm echo} = (2R_S/c)\log(R_S/\ell_{\rm new\,physics})$$

even possible to have signals from the Planck scale. Eg:

$$\ell_{\rm new\,physics} = \ell_{\rm Pl}, \quad M = 60 M_\odot \to \tau_{\rm echo} \simeq 50\,{\rm ms}$$

- quite different from accelerator physics, where the Planck scale is unreachable
- detecting echoes might require SNR=O(100) in the ringdown phase, achievable only with 3G detectors (ET, CE)

Formal birth of the ET Collaboration, Budapest 7-8 June 2022

- Overview
- ET Collaboration Announcement
- Timetable
- Registration
- Participant List
- ET Information
- TRAVEL INFORMATION
- ACCOMMODATION
- Code of Conduct
- GDPR
- Conference photo
- Some more photos

XII Einstein Telescope Symposium

(The birth of the ET Collaboration)

The XII symposium of the Einstein Telescope (ET) took place in Budapest, at the Hungarian Academy of Sciences, on the 7th - 8th of June. The ET scientific community met in Budapest for a crucial step in the long Einstein Telescope journey: the formal establishment of the ET Collaboration.

More than 400 scientists, out of more than 1200 members of the Collaboration, participated in the meeting in person or remotely. The ET members discussed the status of the experiment, the technical challenges, the scientific case, and the scientific and technical progresses made by each of the ET boards. The ET Project Directorate presented the perspective of the funding agencies. Finally, the approved INFRA-DEV Horizon EU project, for supporting the preparation phase of the experiment, and the INFRA-TECH Horizon EU proposal, recently submitted to Brussels for supporting technological R&D activities, were introduced to the whole Collaboration.

The 12th ET symposium is a milestone of the Einstein Telescope project. The ET project is on the ESFRI roadmap since July 2021. A collection of European research institutions, universities and research teams is on the way to establishing the Einstein Telescope Collaboration. That is the primary goal of the